



UNIVERSITÀ DELLA CALABRIA



UNIVERSITÀ DEGLI STUDI DELLA CALABRIA

Dipartimento di **FISICA**

Scuola di Dottorato

Scienze, Comunicazione e Tecnologie "Archimede"

Indirizzo

"Fisica e Tecnologie Quantistiche"

Con il contributo di

Secretaría de Educación Superior, Ciencia, Tecnología e Innovación

(SENESCYT-ECUADOR)

CICLO

XXVIII

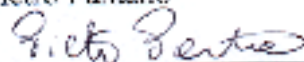
**Environmental Radon Measurements Using a Closed Chamber for Building
Materials and Water and a Feasible Program for Ecuador**

Settore Scientifico Disciplinare FIS/07-FISICA APPLICATA

Direttore:

Prof. Pietro Pantano

Firma



Supervisore:

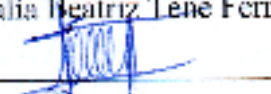
Dott. ssa Marcella Capua

Firma



Dottorando: Dott.ssa Talía Beatriz Lene Fernández

Firma



Environmental Radon Measurements using a
closed chamber for building materials and
water and a feasible program for Ecuador

Talía Beatriz Tene Fernández

February 14, 2017

Contents

Introduction	3
1 Radon fundamentals	5
1.1 Radon discovery and properties	5
1.2 Radon release	9
1.3 Radon transport	11
1.4 Radon accumulation	14
1.5 Radon effects on human health	15
1.5.1 Biologic effects of radon exposure and its RDP	16
1.6 Radon recommendations and laws around the world	19
2 Detectors and methods	22
2.1 Active detectors	23
2.1.1 Detector based on scintillation technique	23
2.1.2 Semiconductor detector	24
2.1.3 Ionizing detector	25
2.2 Passive detectors	25
2.2.1 Continous passive radon detector	26
2.2.2 Electrect ion chamber	26
2.3 Emanometry	27
3 Water and air radon activity concentration measurements	31
3.1 Sampling protocol for radon in spring water	32
3.2 Radon measurements in water	33
3.2.1 Springs investigated in Calabria	33
3.2.2 Measurements performed in Orbo spring	33
3.3 Indoor radon measurements	38
3.4 A protocol for preventive indoor measurements	38
3.4.1 Indoor measurement in a Presila Kinder garden	39
3.4.2 Laboratory background	41

4	Closed Chamber method for volcanic building materials and water assessment	45
4.1	Radon assessment of volcanic building materials	46
4.1.1	Experimental Set-up	46
4.1.2	Detectors and samples	47
4.1.3	Experimental procedure	51
4.1.4	Radon exhalation rate	52
4.1.5	Chamber leakage rate	54
4.1.6	Back diffusion rate	55
4.1.7	Background	56
4.1.8	Results and discussion	57
4.2	An alternative method for radon concentration measurement in water using a closed chamber	61
4.2.1	Experimental procedure	61
4.2.2	Method	62
4.2.3	Results and discussion	63
5	A program to transfer the knowledge to Ecuador	67
5.1	Main features of Ecuador	68
5.2	Objectives and justification	71
5.3	Working plan	73
	Conclusions	74
	Acknowledgments	76

Introduction

Radon is the larger natural source of exposure for population and workers. During the last decades the evolution of the knowledge on the effect of the exposure to radon and its daughters, has allowed the implementation and improvement of appropriate regulations, norms and limits applied to reduce the risk for population and workers, as for example, in the European and North American societies. South America is still in the beginning of the environmental radioactivity researching. In this panorama Ecuador represents a particular case because it has been investing the 2% of GDP (gross domestic product) in research during the last decade. Ecuador has been developing many research projects in different science fields (including environmental research), starting from the professional specialization in experienced Universities around the world. The present document evidences the large radon research activity, still ongoing, developed in Calabria Region and focused to be applied in Ecuador country.

This work covers the relevant results reached in terms of experimental in environmental physics. Part of the work is dedicated to measurements in water and in particular the implementation of a protocol of sampling and a comparison between measurements, methods and techniques. Moreover will be present an alternative method to perform water radon concentration measurements using a closed chamber.

The closed chamber, built in plexiglass, has been projected and realized in the laboratory of Physical Department of UNICAL. It will mainly use to assess the radon mass exhalation rate from volcanic building materials. Building materials can be a relevant source of indoor radon, this is particularly true for volcanic materials widely used in Italy, as example tuff. For this reason we have use volcanic tuff to characterize the closed chamber. The results of the characterization and performance will be shown.

Keeping in mind Ecuador, has been realized the program of my PhD,

supported by Subsecretaria de Educacion Superior, Ciencia y Tecnologia (SENESCYT).The results of this study are a contribution to the research activity around the radon gas, further than this, it represents a preliminary study to develop a radon campaign measurements in Ecuador, contributing to the control of an important source of exposition. Taking into account the particular conditions of Ecuador, makes it an ideal open sky laboratory.

Chapter 1

Radon fundamentals

Natural radon is the only element as noble radioactive gas present in the three natural decay chains in and not uniformly distributed over the earth. The main chemical and physical properties are reported in this chapter, together with the natural mechanism of production and transport to the environment where it can be source of ionizing radiation hazard for humans. In addition, radon health effects and international directives and laws will be brief summarized at the end of the chapter.

1.1 Radon discovery and properties

Radon is the fifth radionuclide discovered after uranium, thorium, radium and polonium. In 1899 at Mc Gill University in Canada, the New Zealand Ernest Rutherford and the British Robert Owens, discovered "the emanation" from thorium: thoron (^{220}Rn) [1, 2, 3]. In 1900 the German chemist Friedrich Ernst Dorn observed a second isotope coming from radium (^{222}Rn) [4]. Then, in 1903 the French chemist André-Louis Debierne discovered that actinium also emitted a radioactive gas (^{219}Rn) [1]. Radon was accepted as a new element by the International Commission for Atomic Weights in 1912, later in 1923, the International Committee for Chemical Elements and the International Union of Pure and Applied Chemistry (IUPAC) approved the use of the names radon (Rn), thoron (Tn) and actinon (An) [5].

Radon is a colorless, odorless and tasteless radioactive inert gas, unstable in all its isotopes [7]. Radon is denser than air and fairly soluble in water. Table (1.1) summarize the mean properties. Although it is a noble gas, radon shows the behavior of a "metalloid"¹. It reacts with fluorine, halogen fluorines, di-oxygenyl salts, fluoro-nitrogen salts, and halogen fluoride-metal [8].

¹an element which exhibits some of the characteristics of metals and nonmetals

Characteristic	Value
Boiling point	-62°C
Melting point	-71°C
Critical temperature	+104.5°C
Critical pressure	62.4 atm
Solution enthalpy	
at 0°C	28.0 kJ/mol
at 35°C	19.7 kJ/mol
Density of gas at standard temperature and pressure	9.73 g/l
Density of liquid phase	0.005-0.006 g/l
Atomic cross section	0.37 nm
Viscosity at 0°C	0.021 Pa.s
Surface tension	2.9 mN/cm
Solubility in water at 0°C	51.0 cm ³ radon/100 cm ³ water
Solubility in water at 25°C	22.4 cm ³ radon/100 cm ³ water
Solubility in water at 50°C	13 cm ³ radon/100cm ³ water

Table 1.1: Rn main physical and chemical properties [6].

But in ambient conditions radon is an inert gas that can easily scape from it source and does not form chemical compounds.

All the three radon isotopes are present in the three natural decay chain, the other elements of the series exhibit different chemical and physical properties in particular: radium as an alkaline earth metal, polonium a metalloid and bismuth, thallium and lead as metals. Radon importance in radio protection lies on their mean lives and relative abundance. Rn-219 is the shortest lived and is virtually always produced in much smaller amounts than is Rn-222, since the natural U-235/U-238 ratio of their progenitors is 0.00719. Hence Rn-219 can be consider negligible in terms of hazard. Also Rn-220 is short lived relative to Rn-222 and consequently reaches smaller distance from its source than does Rn-222. In air, the distance diffused over a mean life is 2.2 m for Rn-222 and 0.029 m for Rn-220 [9, 10]. This work is concentrated to the study of the isotope Rn-222, from now on called radon.

Rn-222 produced by an alpha decay of Ra-226 is $\sim 100\%$ alpha emitter (5,6 MeV) [11], see the figure 1.1. The radon decay products are not chemically inert and in air they give rise to molecules in condensate phase or are attached to airborne dust or water particles. Thus is a radioactive aerosol that could be deposit in the lungs in whole the decay. ²²²Rn is in radioactive

Parameter	Symbol	Rn-222	Rn-220	Rn-219
		Radon (Actinon)	Radon (Thoron)	Radon
Half life	$T_{1/2}$	3.8232 (8) d	55.8 (3) s	3.98 (3) s
Decay constant	λ	2.098E-6 s^{-1}	1.242E-2 s^{-1}	1.742E-1 s^{-1}
Average recoil energy on formation	E_r	86 keV	103 keV	104 keV
Specific activity	Am	5.69E15 Bq/g	34.00E18 Bq/g	478.9E18 Bq/g
Diffusion coefficient in air	D_a	1E-5 m^2/s		
Diffusion coefficient in water	D_w	1E-9 m^2/s		
Alpha energy	Q^α	5590.3 keV	6404.7 keV	6946.1 keV

Table 1.2: Relevant properties of Rn-219, Rn-220 and Rn-222

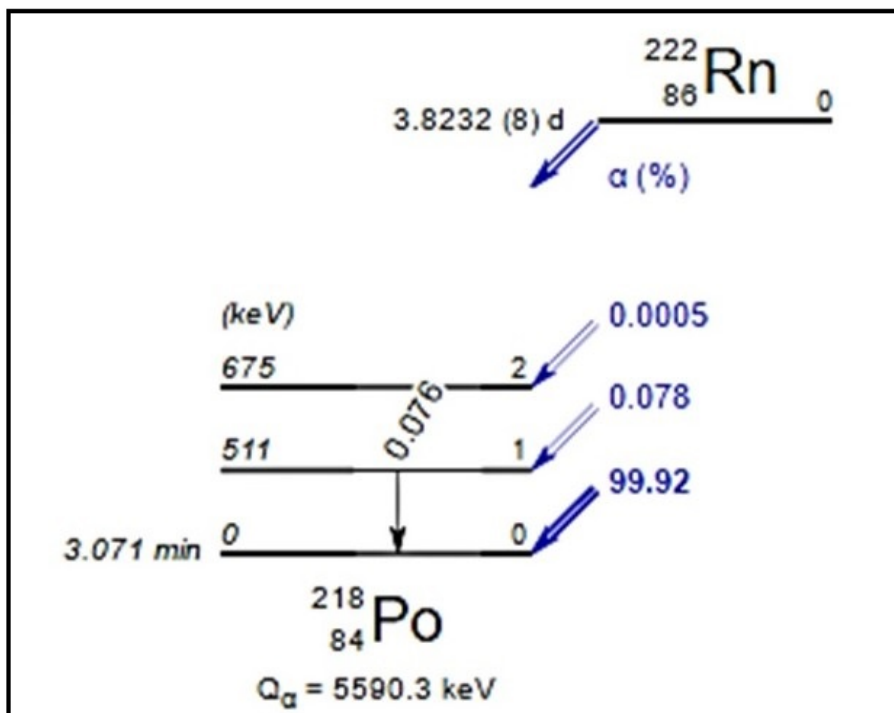


Figure 1.1: Decay scheme of Rn-222.

secular equilibrium with its four short live daughters (^{218}Po , ^{214}Pb , ^{214}Bi and ^{214}Po) after around 3,5 hours. Po-218 and Po-214 are alpha emitters (see fig. 1.2), therefore at secular equilibrium exist three alpha emitters. As is shown in the figure 1.3 , after $\sim 3,5$ hours the activity of Po-218 and Po-214 is equal to the Rn-222 activity.

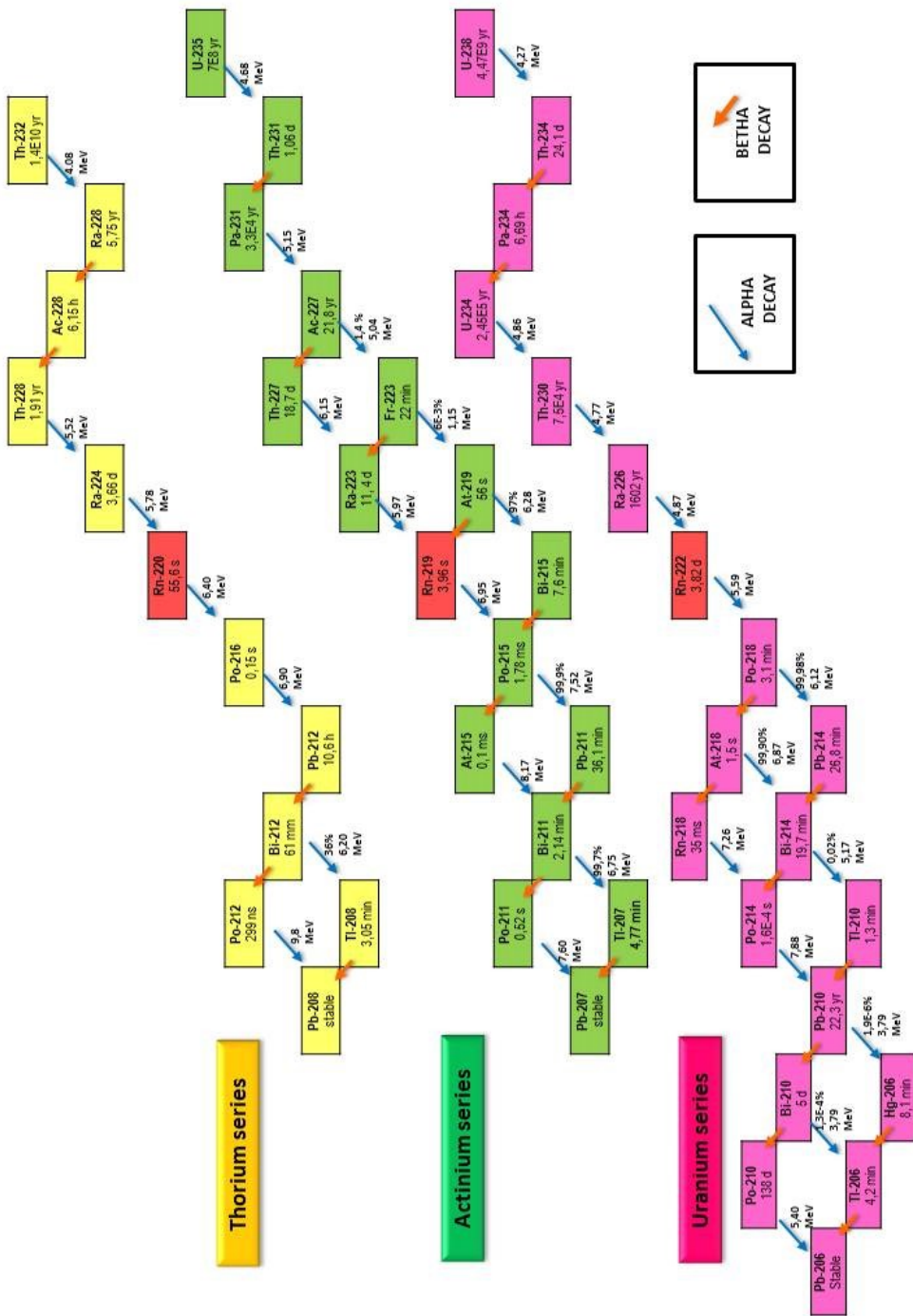


Figure 1.2: Natural radioactive decay chains

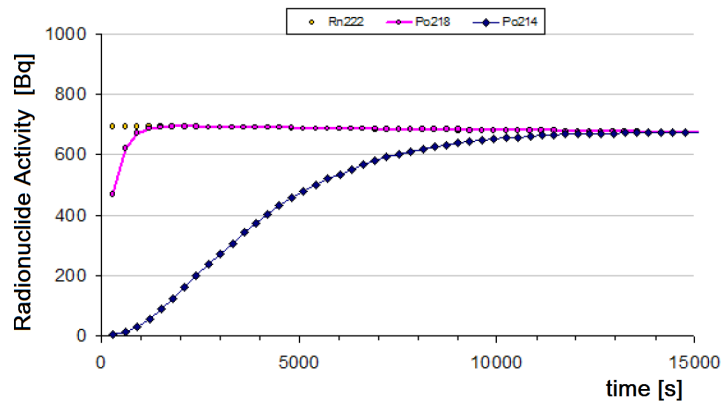


Figure 1.3: Activity of Rn and relatively short live of daughters, as a function of the time.

1.2 Radon release

The origin of the isotopes of radon in the Earth's crust stems on the uranium, thorium and actinium distributed in various amounts on the ground. Uranium, Thorium and Potassium-40 with their radioactive daughters are the greatest part of naturally occurring ionizing radiation in environment [12]. Uranium, thorium and potassium belong to the lithophile group, the elements of this geochemical group occur primarily together with magma rich in silica and remain on or close to the earth surface because they combine easily with oxygen, forming compounds that do not sink into the core. Uranium and thorium can be transported by geological processes to be precipitated in fissures an other permeable structures.

Uranium is the 51st element in order of abundance in the Earth's crust and it is the highest-numbered element to be found naturally in significant quantities on Earth [13, 14]. In nature, uranium is found as ^{238}U (99.2739 – 99.2752)%, ^{235}U (0.7198 – 0.7202)%, and a very small amount of ^{234}U (0.0050 – 0.0059)%. Mineral of commercial value contains several thousand parts per million (ppm) of uranium are ordinarily oxides such as uraninite and carnotite with phosphates and monazite sands [15]. In general ^{222}Rn are produced where ^{238}U is located. Nonetheless, studies suggest to be alert with the climatic (e.g., humid environment) and geologic (e.g., permeable aquifers) conditions, where it is possible for ^{234}U , ^{230}Th , ^{226}Ra , and ^{222}Rn being separated from each other and from the parent ^{238}U . These nuclide are sufficiently long lived to be separated by chemical or physical process from his father. As result of this natural process ^{226}Ra can be dissolved, transported or redeposited elsewhere, then radon is generated far from the

progenitor uranium deposit [16, 17].

Radium 226, the most common isotope, has a half-life of 1600 years. Radium is found naturally in soil, water, plants, food (at low concentration), in rocks (phosphate rock, shales, igneous and metamorphic rocks such as granite, gneiss, and schist, and in common rocks such as limestone) and in uranium ores.

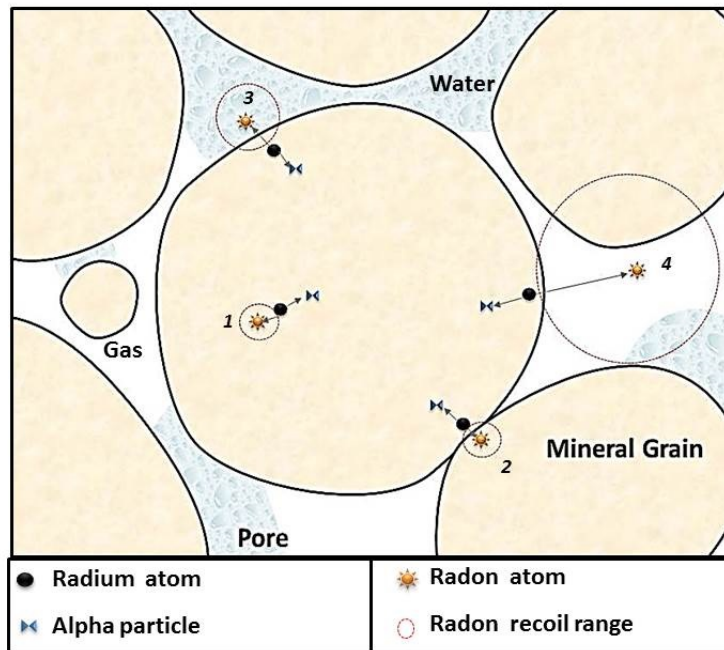


Figure 1.4: Radon emanation from a mineral grains (cf.text).

A fraction of radon originated from radium decay in soil grains is freed to move through the pore space into the atmosphere over land. When ^{226}Ra decays, a ^{222}Rn and an alpha particle are produced. The alpha particle ejection originates the recoil effect on the ^{222}Rn atom. The recoil effect produces the movement of the radon atom from the mineral lattice or molecule where it was created. The distance radon atom can be moved depends on the medium it is released [18]. The mechanisms of radon escapes from grain is illustrated in the figure 1.4, the model describes radium atoms located in a grain with a normal density and surrounded by adjacent grains, porous filled with air and water, then radon produced from radium decay has four destinies [19]:

1. moved trough the originating grain;

2. embedded in an adjacent grain or in another grain in its trajectory;
3. stopped in water;
4. stopped in gas pore.

The distance that radon atoms can be moved (recoil ranges) are: $(0.02 - 0.07)\mu m$ in common minerals, $(0.1)\mu m$ in air and $(63)\mu m$ in water [20], as a consequence only atoms produced at the edge of the grain (less than 70nm) can reach the pore. Measurements developed around the world [21, 22], demonstrate that the most radon produced never escapes from the birth place. The small fraction of radon is available for being transport at scale larger than the pore diameter is defined as radon emanated.

Further than the radium content, radon emanation depends on the features of the material, such as the composition and size of the grains, the distribution of the grains at the internal of the material, the porosity and on the environmental parameters. The environmental parameter like temperature and pressure have a low influence on radon emanation, although a high increasing of temperature may reduce the physical adsorption of radon onto soils [20]. Meanwhile, moisture content has been demonstrated to have a large effect on the emanation of radon from grains. Many studies shown that emanation is much lower when the source material is dry rather than humid, see an example in figure 1.5 [23]. The explanation for this phenomenon may lie in the lower radon range in water compared with air.

1.3 Radon transport

Radon is chemically inert, this fact has important implications on transport. Radon atoms can migrate far from the site of generation by two basic process, diffusion and convection. Convection depends on pressure gradient, which may or not be present. The mechanism responsible of creating this pressure gradient are wind interaction with soil and heating [24].

About diffusion, assuming radon is a fluid, it follows the Fick's law. Under the assumption of steady state, Fick's law postulates that the flux j , goes from regions of high concentration to regions of low concentration, with a magnitude that is proportional to the radon concentration gradient (see fig. 1.7). The fluctuating flow u' in one direction is compensated by another flow u' of same magnitude in the opposite direction. Then one dimensional diffusion flux equation is:

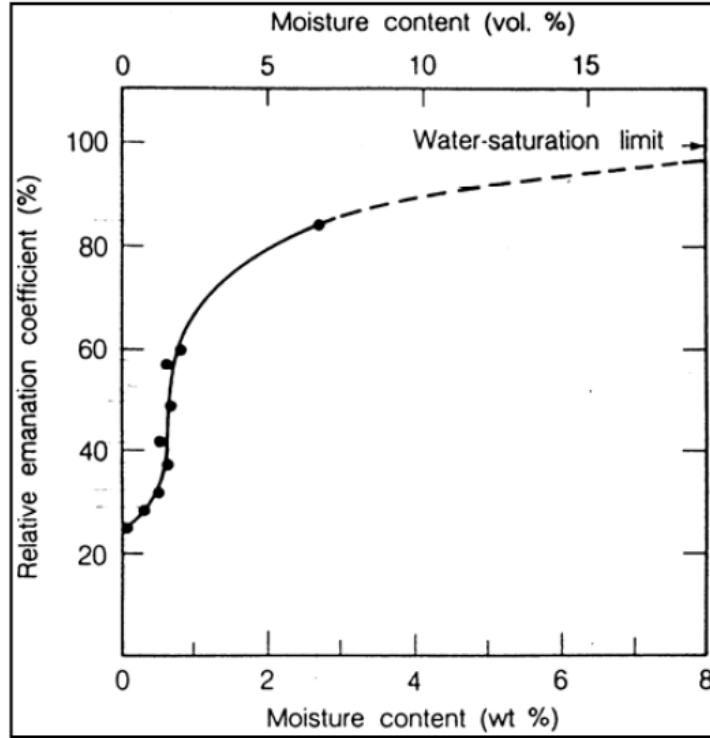


Figure 1.5: Emanation coefficient variation in a material in relation with different percents of moisture [23].

$$j = c_1 u' - c_2 u' = -u' \Delta c \quad (1.1)$$

j dimension is amount of radon per unit area per unit time, c is the concentration of radon shown in fig.1.7. Considering an infinite slab of material, radon diffusion can be described with the diffusion coefficient D which depends on the temperature, viscosity of the fluid and the size of the particles. $c(x)$ is the activity concentration of radon.

$$j = -D \frac{\delta c(x)}{\delta x} \quad (1.2)$$

A large interest is for radon exhalation of building materials or walls. The majority of the emanated radon gas will be exhaled from the surfaces to the environment [26], radon diffusion takes places mostly along the shortest

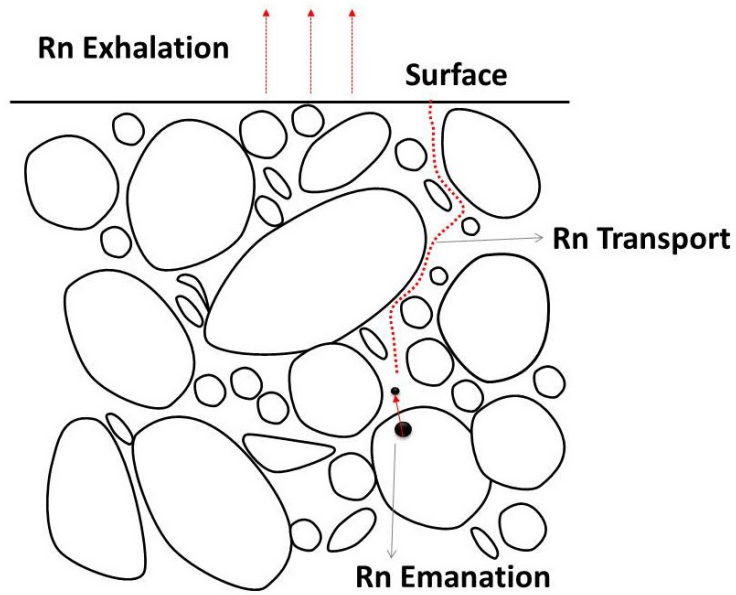


Figure 1.6: Process of radon transportation to be released in the atmosphere.

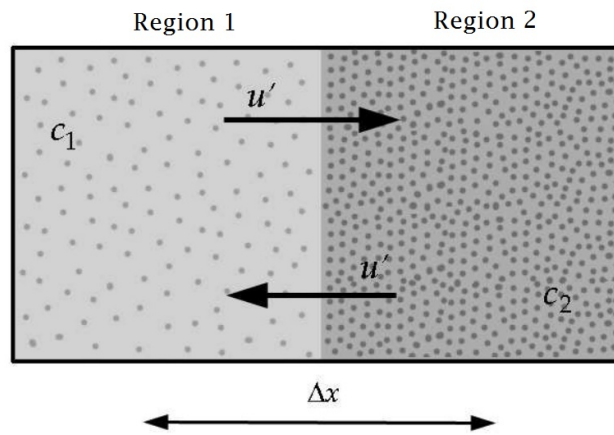


Figure 1.7: Scheme of one dimensional diffusion between two regions with different density.

dimension, its depth. The mass balance on an infinitesimal stretch of a one-dimensional system is sketched in the figure 1.8, where radon is not only diffusing but also is renewed and decay over the time, yields:

$$V \frac{dc}{dt} = j(x, t)A + S - j(x + \Delta x, t)A - \lambda_{Rn} V c \quad (1.3)$$

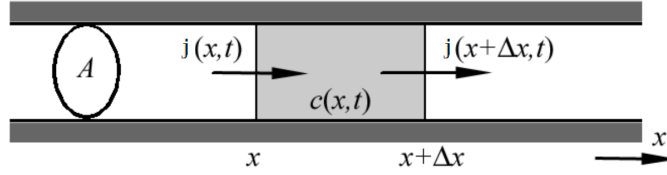


Figure 1.8: Infinitesimal control volume in one dimension [25].

Where $V = A\Delta x$ is the volume of the stretch under consideration, λ_{Rn} is the radon decay rate, and S is the radon source. Dividing by V :

$$\frac{dc}{dt} = -\frac{j(x+\Delta x, t) - j(x, t)}{\Delta x} - \lambda_{Rn}c + s \quad (1.4)$$

where $s = S/V$ is the source per volume. In the limit of an infinitesimal control volume ($\Delta x \rightarrow 0$), this budget becomes a partial differential equation:

$$\frac{\partial c}{\partial t} = -\frac{\partial j}{\partial x} - \lambda_{Rn}c + s \quad (1.5)$$

Using the equation of the diffusive flux 1.2, the general equation that govern the spatial and temporal variability of the radon concentration distribution is:

$$\frac{\partial c}{\partial t} = -D\frac{\partial^2 c}{\partial x^2} - \lambda_{Rn}c + s \quad (1.6)$$

1.4 Radon accumulation

The fraction of radon gas from the soil or from building materials that reach the surfaces and is spread in the environment (exhaled radon) can be accumulated in closed places. The accumulation can occur especially in indoor places or where the air interchange is low, as example, underground rooms, caves, closed mines, isolated buildings, etc. The indoor radon concentration varies largely since high variability of radon rate from soil, building materials and water supplies.

During transport, radon attenuates by radioactive decay, for which reason radon entering buildings usually originates from the upper few meters of the soil. Soil is the major source of indoor radon, pressure gradient is the

dominant transport mechanism of radon coming from soils into most homes with elevated indoor concentrations [2, 27, 28, 17, 20]. Talking about building material, the importance of them as radon source is given by the exhalation rate, defined as the radon activity released per unit of mass or surface of the material, part of this work is dedicated to calculate the values for volcanic building materials. It will be detailed in the Chapter 4. About indoor radon coming from water supplies, it's necessary a very high radon concentration in water to get a significance contribution. High radon concentrations in water are more probable in natural springs, underground water and wells. Results of water measurements carried out in some Calabria springs will be detailed in the chapter 3. Moreover, an alternative method to determine the radon concentration in water will be detailed in the second part of chapter 4.

1.5 Radon effects on human health

The health hazards of radon is not mainly due to it self directly. Radon gas is inhaled but the most part of it is exhaled due to its lifetime is relative long compared with the breathing time and it can not be accumulate in the respiratory system. Besides, inhaled radon does not get close to radio sensitive cells, hence the dose from alpha particles is small [29].

The real risk is produced by its first four descendants 218-Po, 214-Pb, 214-Bi and 214-Po . They are also radioactive and are collectively referred to as *radon decay products* (RDP). They are all metals and have half-lives ranging from a fraction of a second to 27 min. They can be easily condensed on a solid or liquid surface and can be attached to aerosols or remain suspended in air as free atoms. A person can inhaled them and they are transported by the respiratory system, depending on breathing patterns and the aerodynamic size of particles with which the RDP are associated. Since their short half lives, RDP are deposit on epithelial surfaces within the lungs and they will completely decay. The sensitive bronchi surface can be irradiated by the alpha particles. Alpha particles can transfer considerable amounts of energy. The collective RDP concentration is usually represent in terms of total energy that would be released by alpha particles when all of them decayed completely. This quantity is called potential alpha energy (PAE) and the concentration (PAEC) is measured in units of energy per unit of air volume [Jm^{-3}]. The most ionizing and short range alpha particles are those from polonium isotopes: 214-Po and 218-Po.

Early evidences of Radon effects on miners. About 500 hundred years ago, *Paracelsus* and *Agricola* reported a high mortality due to respiratory

disease in miners of Central European silver mines and in mercury ores respectively. The real nature of the affection was not discovered, until 1879, when *Härtling* and *Hesse* by clinical and anatomical research, proved it to be a malignant tumor of the lungs [5]. The first case of lung cancer in a radium factory worker was observed in 1926 by *Pirchan*, who in 1932 described pulmonary cancer cases in miners from the Erz Mountains and concluded that radon was the most probable cause of the tumors [30]. At the same time in United States many studies were carried out cross in mines located in four states of Arizona, Colorado, New Mexico and Utah, concluding that the excess respiratory cancer rates among uranium miners were not attributable to age, smoking activity, heredity, urbanization, self selection, diagnostic accuracy, prior hard rock mining or ore constituents. They attributed the excess risk to airborne radiation . Making a summary there is a direct implication between the inhalation of RDP and lung cancer in underground miners.

Like in mines, radon can be accumulated in enclosed environments like public, working and residential places, as consequence exist a significant hazard from radon exposure in these indoor sites . To present preliminary information about risks from indoor exposure to radon and its daughters were used extrapolation from miner studies. Actually exists important observational studies between residential radon exposure and lung cancer. The most cited authors [31, 32, 33, 34, 35] have presented in their studies the direct evidence of an association between residential radon and lung cancer risk. In particular Darby et al. analyzed 13 european case-control studies and found a linear dose-response relationship, with no evidence of a threshold dose. He concludes that the hazard from residential radon, is particularly for smokers and recent ex-smokers, and it is responsible for about 2% of all deaths from cancer in Europe [36].

1.5.1 Biologic effects of radon exposure and its RDP

Radon represents a risk primarily for the respiratory system, however, two other potential hazards have been identified. Studies suggest that the water ingestion with a particularly high level of radon can lead a significant risk of stomach cancer. And other studies suggest that deposition of RDP on the skin may be capable of irradiating sensitive basal cells [37].

Al low radon exposure conditions, found in residential environments, the biologic effects of radon is initiated by the passage of single alpha particles with very high linear energy transfer (LET). The alpha particle tracks ionizes multiple sites of DNA, it yields in removals and and rearrangements of

chromosomal regions and lead to the genetic instabilities implicated in tumor creation and progression. Low exposure is quantify for the number of cells exposed rather than in the amount of damage per cell.

Ingestion

About radon ingestion exist experimental evidence, in 1965 a historical human experiment was performed. Two subjects on two occasions drank radon plus its daughters dissolved in 100 ml of water [38]. In addition have been proposed biokinetic models for ^{222}Rn body absorption and distribution following drinking water ingestion, the prediction of this model is well compatible with the human data for the whole body retention following ingestion of ^{222}Rn in water on an empty stomach [39]. Supported by these and many others studies about radon ingestion can be conclude that: ingested radon is absorbed from the gastrointestinal tract and readily eliminated through the lungs. In the case of ingestion, the stomach receives a much higher dose than any other organ. The dose deposited in the stomach depends on time length of time that ingested radon remains there and how radon is diffused by the walls. If radon has entered the blood, through either the stomach or the small intestine, it is distributed among the organs according to the blood flow to them and the relative solubility of radon in the organs and in blood. Radon dissolved in blood that enters the lung will equilibrate with air in the gas-exchange region and be removed from the body [29].

The general observations mentioned before have been verified by pharmacokinetic model to describe the ingested radon distribution in the body. The model uses the blood-flow model propose by *Leggett* and *Williams* and the relative solubility of radon in blood and tissue to determine the major tissue of deposition (which is adipose tissue) and retention within this tissue. The diagram of the transfer of ingested radon from the gastrointestinal tract into and through the body is evidence in the figure 1.9. Where the compartment "Large Veins" represents the venous blood return from the systemic tissues, "Right Heart" and "Left Heart" the content of the heart chambers, "Pulmonary" the blood-exchanging gases in the lung, and "Large Arteries" represents the arterial blood flow to the systemic tissues. The compartment labeled "Gut Cont" is the gastrointestinal track that content four segments, the stomach, the small intestine, the upper large intestine, and lower large intestine. The figure 1.9 describe ingested radon is readily distributed through the circulatory system radon by the organs and appears promptly in exhaled air. The results calculated by the described model are consistent with the observations reports is the experimental studies reported in the reference [38].

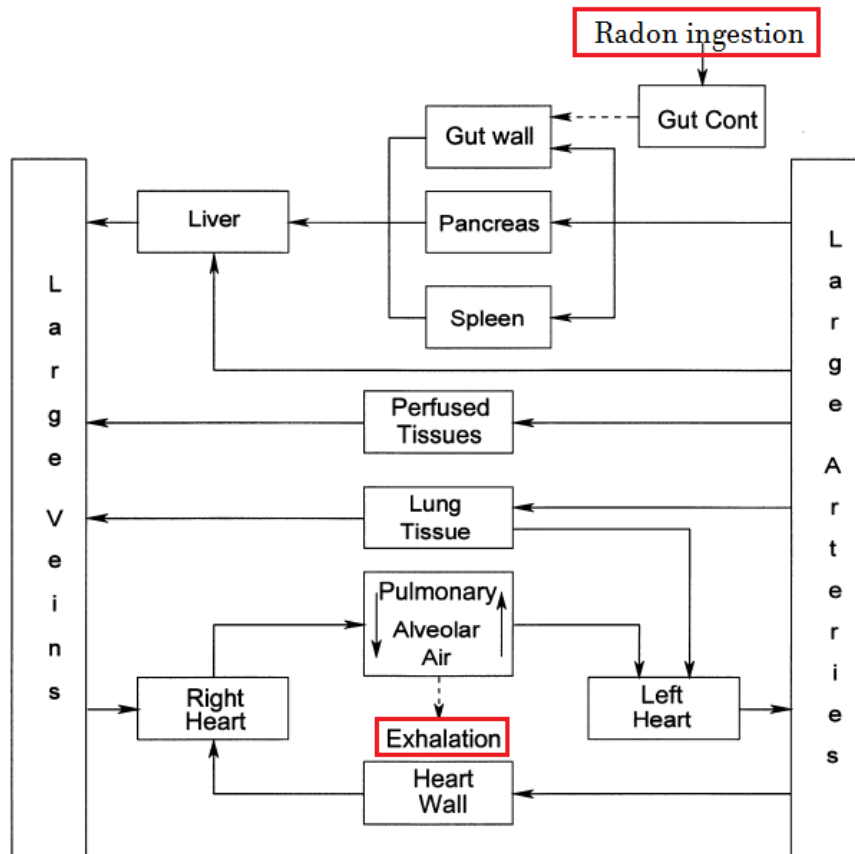


Figure 1.9: Diagram of the probable ingested radon transfer from the gastrointestinal tract into and through the body. Dashed arrows denote the transfer of radon as a gas, and solid arrows correspond to the flow of radon dissolved in arterial (thicker arrows) and venous blood [40].

Other risk from the ingestion of radon have been proposed by Robbins and Harley (see reference [41]). As result of the ingestion of water with radon during the pregnancy, ingested radon can be transported by the blood and diffuses throughout the body including into the placenta thereby alpha-particles emitted by radon and/or its RDP can reach the embryo/fetus. The prenatal exposure during the first weeks represent the most risk for severe effects from radiation. The very small size of the embryo should yield a commensurately small target for alpha-particle hits, but conversely, alpha-particle damage to nuclear DNA may have major consequences

Inhalation

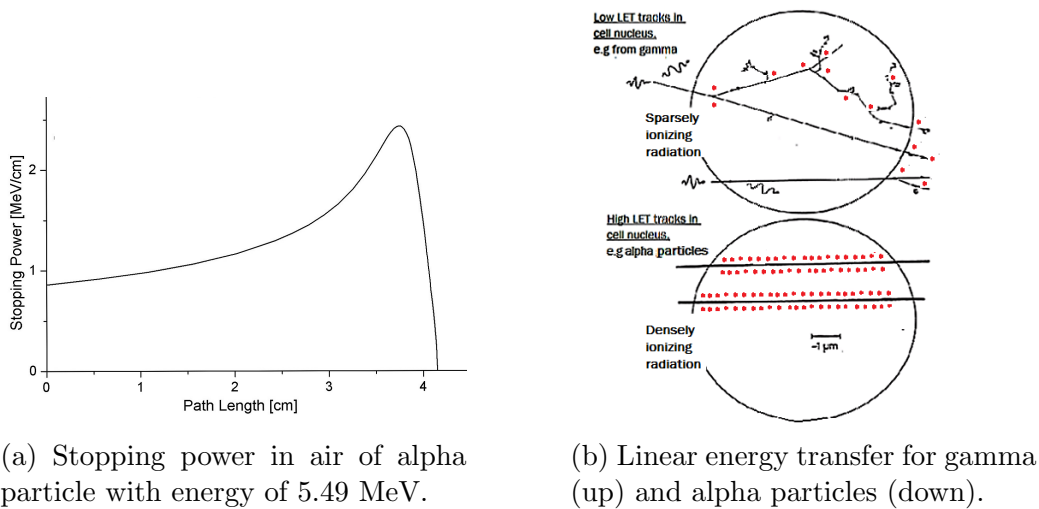
The mean health risk stemming from the exposure to radon arises from the inhalation of its RDP and the consequent dose to critical cells of the respiratory tract[42]. The alpha particles from RDP condensed and attached to the aerosol, travel through the airways and are deposited on the target cells in bronchial epithelium, consequently lung cancer associated from exposure to radon and its decay products is bronchogenic.

For a given target cell under RDP exposition, the practical possibilities can be either to receive an instantaneous large energy deposition, to receive a small number of large energy depositions, each well separated in time by months or years or, do not be irradiated. Alpha particles, which produce a high density of ionizations losing all their energy along a short path (fig.1.10a), in other words, particles with high linear energy transfer (LET), differ greatly from the low LET radiations, such as indirect ionizing gamma rays in their microscopic, spatial, and temporal patterns of interactions with the cell nucleus, subcellular structures, and molecules (see fig.1.10b). The damage produced by alpha particles is concentrated in a relatively small number of densely ionizing track. In addition, in the case of alpha particles, more of the individual damage is due to direct ionizations in the DNA[29]. The localized DNA damage caused by the dense ionizations from high LET radiation is more difficult to repair than the diffuse DNA damage caused by the sparse ionization from low LET radiation.

To estimate the alpha-particle dose delivered to the target cells in the bronchial epithelium per unit radon exposure is necessary to analyse the information of the aerosol size distribution, the unattached fraction of RDP, breathing rate, fractional deposition in the airways, mucous clearance rate and location of the target cells. These parameters including their uncertainties and other particularities (find more details in UNSCEAR 2000 Report) are part of the dosimetry models used to estimate the radiation dose arising from the inhalation of airborne radioactive material.

1.6 Radon recommendations and laws around the world

Radiological protection regulation tends to homogenize in all countries around the world. They incorporate the same criteria and basis of minimum technical parameters, but do not have the same legal formulation as it is of national



(a) Stopping power in air of alpha particle with energy of 5.49 MeV.

(b) Linear energy transfer for gamma (up) and alpha particles (down).

Figure 1.10: The right picture shows the alpha particle crossing the cell in less than 10-12 seconds and delivering to it a large localized energy. Alpha particles produce more large clusters of multiple ionizations within the DNA and in adjacent molecules than do gamma rays. The left graphic draws the Bragg curve of a radon alpha particle, which represent the energy loss of the particle during its travel through the air. The 5.49 MeV alpha particle have lost its energy at 4.14 cm

jurisdiction. Even though this trend, there are still serious differences in regulations between countries specially about radon levels in working and residential places.

In 1988 the International agency for research on cancer (IARC), which is part of the World Health Organization (WHO), classified radon as a Group 1 human carcinogen. The United States Environmental Protection Agency (EPA) lists radon as the second leading cause of lung cancer and the number one cause of lung cancer among non-smokers, estimating it is responsible for about 20,000 lung cancer deaths every year. EPA recommends that all homes should be monitored for radon, and strongly recommends action for any dwelling with a concentration higher than 148 Bq/m^3 , and encourages action starting at 74 Bq/m^3 .

The European Atomic Energy Community (EURATOM) on its Directive 2013/59 recommends that action should be taken starting from concentrations of 400 Bq/m^3 for older dwellings and 200 Bq/m^3 for newer ones. Re-

cently, Health Canada proposed a new guideline that lowers their action level from 800 to 200 Bq/m^3 . The World Health Organization has recommended a radon reference concentration of 100 Bq/m^3 for indoor residential places.

For radon concentration in drinkable water, the World Health Organization issued as guidelines (1988) that remedial action should be considered when the radon activity exceeded 100 Bq/l in a building, and remedial action should be considered without long delay if exceeding 400 Bq/l . The present thesis use the new Italian regulation (D.Lgs. 28/2016) based on the new EURATOM Directive that impose the maxim limit for domestic water is 100 Bq/l .

Ecuador is a particular interest of this thesis. The institution of the radio protection regulation in Ecuador is the Subsecretaria de Control y Aplicaciones Nucleares (SCAN). Ecuador does not have laws to control the exposition of the population to radon, in general the unique document available is a *Regulation to control and moderate the pacific use of ionizing radiation in Ecuador (1979)*, published on the web site of the SCAN. This document is dedicated only for the use of radiation ionization in medicine and briefly in industry. Any paragraph of this Regulation indicates which are the guidelines for environmental ionizing radiation, especially radon.

Chapter 2

Detectors and methods

Depending on the purpose of the measurement, and taking into account the experimental condition and environmental parameters. In the detectors and tools used in this thesis for air or water radon concentration of activity are present.

2.1 Active detectors

Detector commonly known as active allows a fast collection of radon and/or its daughters by forcing the entering of the gas into the detector. They are generally used for measuring at short time in continuous monitoring.

2.1.1 Detector based on scintillation technique

Alpha particles emitted by radon decay can be detected when they interact with scintillation material producing luminescence [43, 44]. Henry F. Lucas used this scintillation technique to built a steel shell internally coated with silver activated zinc sulphide ZnS(Ag), to detect alpha particles. This detector is known as Lucas or scintillation cell.

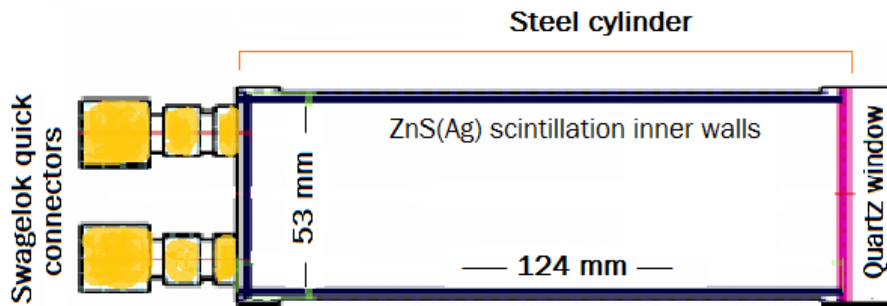


Figure 2.1: Cilinder Lucas cell.

The scintillation cells available in our laboratory (fig.2.1) have a volume of 270 ml, they are assemble with a transparent quartz window coated with a tin oxide at one end and two swagelok connectors at the other end to fill the cell with sample of air. The high efficiency scintillation material for alpha particles, silver activated zinc sulphide, is an inorganic polycrystalline powder transparent to its own scintillation light¹. The light emitted is isotropically spread out and only a fraction of the light is collected by a photomultiplier interfaced with the detector.

When the Lucas cell is interfaced, for example, with the photomultiplier contained in the AB-5 monitor the scintillation photons are converted into electrical signal and then converted in counts. The cell efficiency depends

¹Thickness greater than about $25\text{mg}/\text{cm}^2$ shows opacity to its own luminescence

on the geometry of the cell. The cells used in this thesis have an efficiency about 75% and sensitivity of 0.051 cpm/Bq/l. The efficiency can be reduced by humidity and background of long lived elements of the radon chain, in particular ^{210}Po . For this reason a frequent Cell calibration and a background evaluation is needed. Studies on the quality of the correction has been reported in [45]

2.1.2 Semiconductor detector

The interaction between a charge particle and the valence electrons of the semiconductor detector originates a physical process called *electron hole pair*. These electron hole pairs are the information carriers created along the path taken by the charged particle through the detector. Even in the absence of ionizing radiation, all semiconductor detectors will show some finite conductivity and therefore a steady state of "leakage current" can be observed. To avoid this significant source of noise an alternative method of "doping" at the surface of the semiconductor is to expose the surface to a beam of ions. This method is known as ion implantation. A particular method of silica detectors fabrication combines the technique of ion implantation and photolithography to produce detectors know in the market as **passivated ion planar silicon detector**, which have very low leakage currents and excellent operational characteristics to obtain a superior energy resolution [43, 46].

A passivated ion planar silicon detector, combined with an electrostatic collection of radon and its alpha emitters daughters is used in the radon gas monitor RAD7 produced by Durrigde Company (see fig. 2.2) [47]. The system allows to measure radon and thoron using a spectral energy analysis, discriminating between the energy of alpha particles. RAD7 monitor uses only the polonium-218 signal to determine radon concentration, and the polonium-216 signal to determine thoron concentration. The detection limit of the apparatus is equal to 0.01Bq/h for radon and 6Bq/h for thoron [48]. This detector allow to collect information about the temperature and relative humidity during the radon measurement.

Due to the sensivity to the humidity, RAD7 should work with a relative humidity lowe than 10% (8 if it possible). Hight humidity improve the neutralization of ^{2218}Pb from water molecules, reducing the efficiency of the detector. A dedicated software, produced by Durridge, correct for this effect.

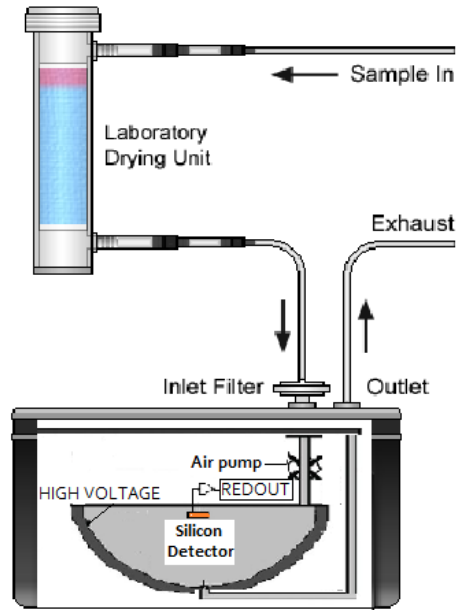


Figure 2.2: RAD7 setup radon measurement in air.

2.1.3 Ionizing detector

The operating principle of ionization chamber is the ionization process of a gas. A particular model of ionizing chamber is presented under the name of AlphaGUARD Radon Monitor [49]. AlphaGUARD radon monitor has a total volume of 0.62 l and the active volume is 0.56 l. In the air entrance it has a filter made of glass fiber to retain the radon progeny. The sensitivity of the detector is 1 cpm at 20 Bq/m^3 . Like RAD7 this detector allows to collect temperatures and relative humidity information of the measurement. The detector offers results in terms of radon concentration or activity.

2.2 Passive detectors

In the passive detectors, radon enters by diffusion mechanism [9]. They are useful for measurement integrated over a long time periods. Lucas Cell can be used as passive detector, Continuous Passive Radon Detector (CPRD) is a particular scintillation cell provided by PYLON Electronic development company that is used with the AB-5 monitor. AlphaGUARD ionizing chamber, works in optimized diffusion and is considered as passive detection. Besides them the electret ion chamber is definitely considered as passive detector.

2.2.1 Continous passive radon detector

The CPRD is a particular scintillation cell provided by PYLON Electronic development company [50]. This passive scintillation cell is a metal cylinder with four holes at one side and it's opened at the other. The four small holes have a light proof polyurethane foam barrier and the open end fits against the photomultiplier contained in the AB-5 Pylon. Air diffuses through the barrier and it is deposited inside the cylinder, then alpha particles, coming from the radon decay, follow the same scintillation process, photon collection and electrical signal counting detailed in the subsection 2.1.

About especification: the CPRD alpha energy range coverered is (45 ± 9) and the sensitivity 0.041 cp/Bq/m.

2.2.2 Electrect ion chamber

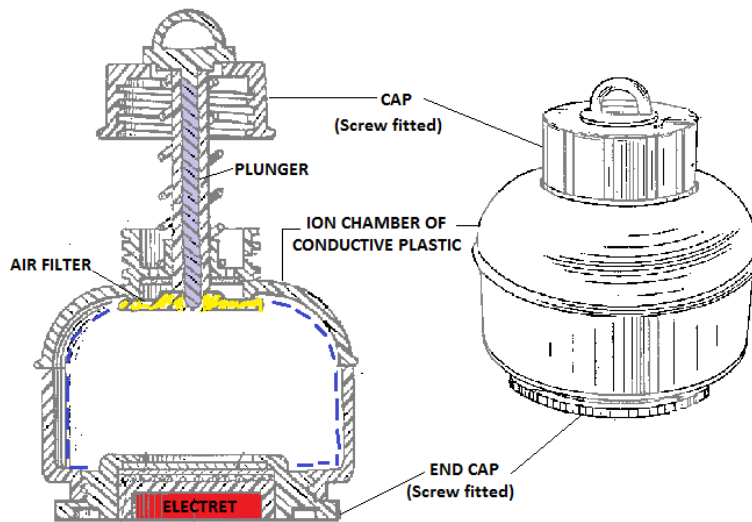


Figure 2.3: Electrect ion chamber diagram . On the right side the chamber is closed and in the left side is ready to start a measurement [51].

An electret ion chamber is a particular sort of ionization chamber, it consists of a small cup or canister with a permanent electrostatic field provided with an electrete at the bottom, a filter inlet is present at the top (see fig.2.3).

The ^{222}Rn enters easily through the filter, when it decays inside the chamber emitting an alpha particle that can generate ionization, ions are

collected by the positive charged electret. The reduction of charge (or surface potential) on the electret is proportional to the number of ions collected [52, 53].

They can be used for preliminary short-term (few days) measurements or long term measurements (months) with detection limit per day of 10 KBq/m^3 and 700 KBq/m^3 respectively.

An Electret Passive Environmental Monitor (E-PERM) [54] has three components: a positively charged teflon disk (electret), a plastic chamber and a portable electret voltage reader. The surface potential electret reader (SPER1) is the voltage reader suitable for relatively small numbers of electret measurements [55].

The radon concentration is determined by ,

$$C_{Rn} = \left(\frac{\Delta V}{CF \times t} - Bg \right) H \quad \left[\frac{Bq}{m^3} \right] \quad (2.1)$$

measuring the initial and final voltage difference ΔV , the time of exposition t , the calibration factor CF that is related to the linear voltage drop and depends on the configuration chamber/electret, the correction factor, H owing to the height where was determine the measure and the measurement background Bg which is generally due to the gamma cosmic rays and terrestrial radiation.

2.3 Emanometry

The emanometry is a method for the determination of radon-222 activity concentration in a water sample, allowing the transference of radon from water to air fluxing (bubbling). The radon transferred from water to air can be easily detected with the Lucas cell or RAD7 detector, already presented. To maximize the degassing efficiency, an adequate air flux and time of fluxing have to be choose. Three degassing systems are available in our laboratory: the degassing system proposed by Pylon with a extraction efficiency of 95% $\pm 5\%$, the degassing system of Mi.am s.r.l. and the RAD H_2O degassing kit. About the last two tools the efficienfy of extracting is not defined separately

The Pylon degassing tool (see fig. 2.4 extracts radon from water thanks to fluxing air through a porous stone submerged in the water sample. Gas radon extracted from a sample of water with Emanometric technique and

transferred to the Lucas cell, allows to measure the concentration of activity of the sample of water. The concentration of activity in a sample of water, degassed and transferred in a Lucas cell can be measured

$$C_{Rn} = \frac{Nett\ count}{V_{H_2O} f \epsilon} K \alpha \quad (2.2)$$

Where the *Nett count* is number of counts after the cell background subtraction, V_{H_2O} is the volume of the water sample, ϵ is the cell efficiency, f is the degassing efficiency, K is the time correction between the sampling and measuring time and α is equal to 1/3 if the measurements are performed after the secular equilibrium (3.5 h). The Mi.am degassing kit is more efficiency in terms on time spent because it allows the measurement just after the degassing correcting for the disequilibrium.

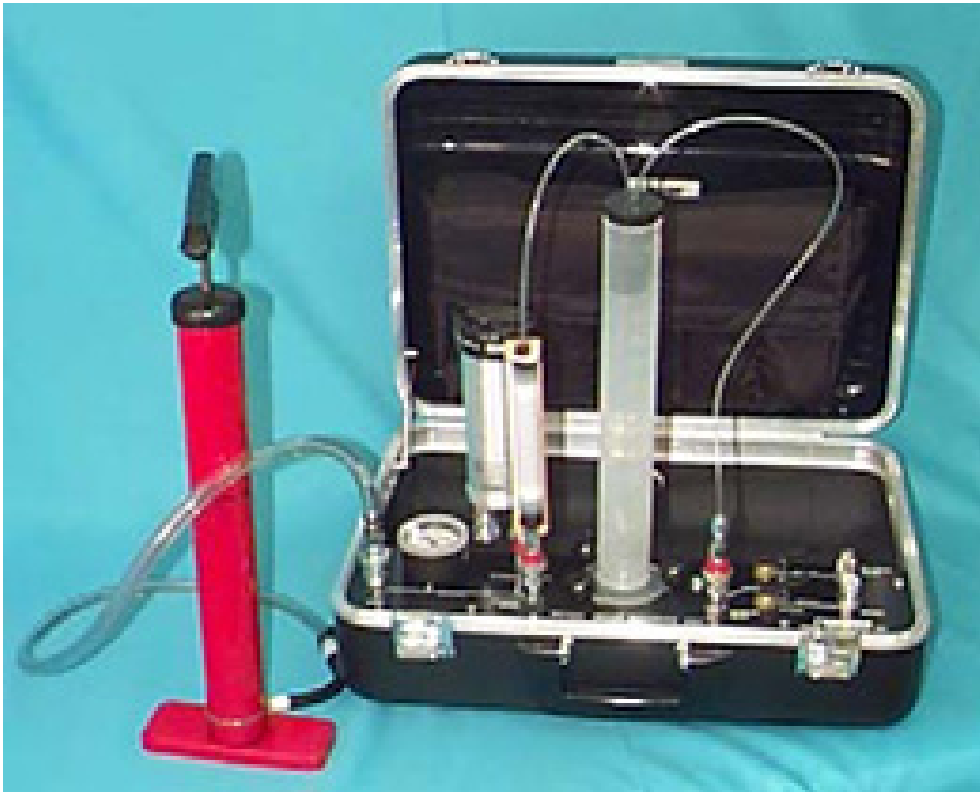


Figure 2.4: Pylon degassing tool.

To obtain the radon concentration of a water sample an alternative tool is presented by DurrIDGE company [56]. The RAD H₂O water accessory contains

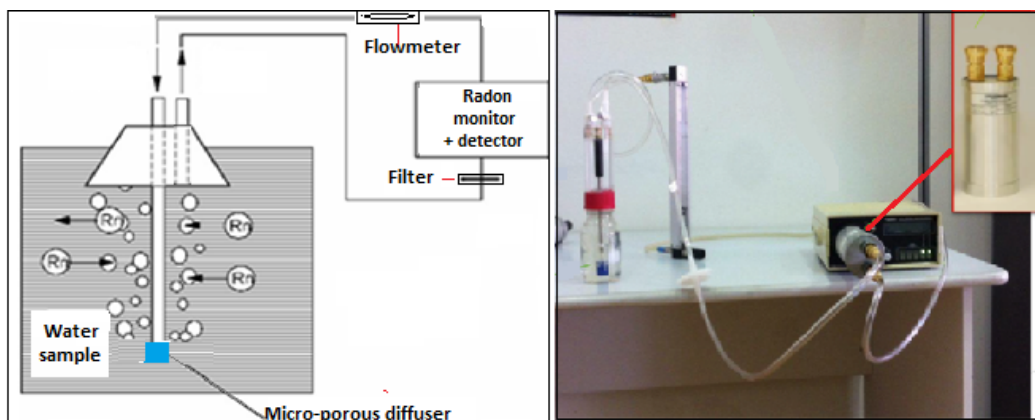


Figure 2.5: Sketch (right) and experimental setup for radon water measurement, using the Rn kit interfaced with the Lucas cell and AB-5 Pylon monitor.

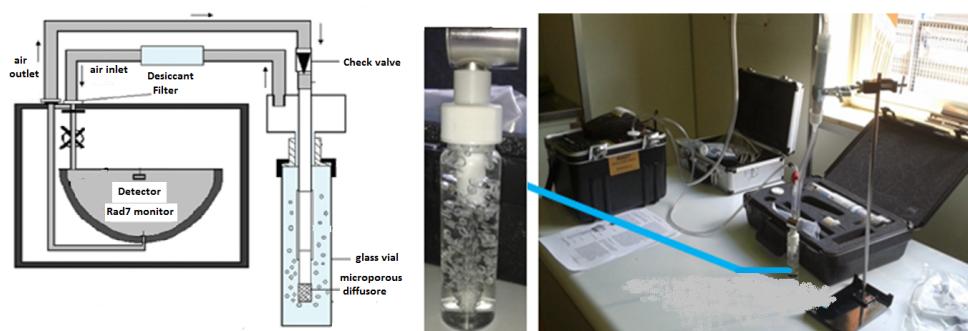


Figure 2.6: (Left) Schematic RAD H₂O setup of a radon water measurement. (Right) Extraction of radon from a water sample using the system RAD H₂O/RAD7 monitor.

the glass vial with micro-porous stone, the desiccant, the desiccant support stand, tubing and filters. This tool offer two options: a vial of 250ml for radon concentration lower than 110 Bq/l and a 40ml vial for higher concentration. To perform a measure is necessary to create a closed loop including the RAD H₂O and the RAD7 monitor, it makes the air flows through the system, the micro-porous stone produces a bubbling inside the water, this effect causes the radon exhaust from water and bring it to the silicon detector contained in the hemisphere cell before passing by the desiccant and filters in order to avoid the humidity and other contaminant particles. A typically measure

takes about 30 minutes, without taking in account the time to purge the detector. If the air humidity is relatively high the purging can requierd various hours.

Chapter 3

Water and air radon activity concentration measurements

Regarding measurements on public water and taking into account the new Italian regulation (D.Lgs. 28/2016) laying down requirements for the protection of the health with regard to radioactive substances (included radon) in water intended for human consumption. We have improved the protocols of sampling and measurement in spring water. In this chapter will be presented the results obtained. Additionally this chapter the results obtained from indoor measurements will present. The results obtained for indoor measurements will be also presented. Some of the results of radon in air represent an important information for the exhalation building material measurements shown in the next chapter.

3.1 Sampling protocol for radon in spring water

The radon water measurements are focused on samples of drinking water coming from aquifers. The radon measurements in water with Emanometric technique involves three steps: the sample collection, the radon extraction from water and the radon counting.

Radon tends to leave water when is in contact with air, specially if the water presents a low salinity or if it is heated or agitated [57]. During the sampling all these conditions can occur, then the sampling technique is generally the major source of error in measuring the radon content in water [56], increasing the total uncertainty up to 8% [58, 59]. The guidance followed to collect a sample adopted in this work is described below.

Regarding to the source, previous investigations on the concentration technique, age of the fountain, water pretreatment, etc. can help to qualify the source. If the fountain is manipulated upstream the measurement can be not useful to qualify the radon concentration at the spring, but only to quote the concentration at the exit. During the water collection, to avoid degassing, the bottle must be places as near as possible to the tap of the fountain. The bottle inclination reduces the bubbling during the sampling. Before the sampling the flow rate, water and air temperature and meteorological conditions (in particular humidity and rain) must be registered.

Regarding to the bottles and taps, to avoid the presence of bubbles in the sample water, the bottles should be made of glass or rigid plastic to avoid the deformation during the manipulation, the bottle cap could include an internal teflon disk. Bottle caps must fit precisely with container to prevent water spillages. The container needs to be previously cleaned and dried.

Is a usefull practice to fix securely a sample label with a unique sample number to identify the containers. Record clearly the sample number, location (address/name of the source), date, time, sampler.

At least three samples per time should be collected. And the measurement must be repeated one time per season, before to quote an average radon concentration activity in spring water.

Depending on the measurement apparatus the samples will be degassed following the appropriate procedure, that depends on the detector used, as explained in the previous chapter.

3.2 Radon measurements in water

The aim of the measurements in water is to optimize a protocol of measurements to make a complete analyses of the groundwater springs in Calabria taking into account only which of them are available and frequently used from the population.

3.2.1 Springs investigated in Calabria

The first step has been to select public springs. It has been done starting from the only available list of water sources, elaborated in 1941 by the Public Work Minister of Italy. But a large fraction of them actually does not exist due to the anthropization or natural modifications of the area where was located the spring. To extend the list, sources suggested by local people also were included in the study. For each source were identify the geologic characteristics of the place where the sources is located e.g. type of rocks, geological faults, known indoor radon concentration of surroundings places, technical information of the fountain, etc. as request from the sampling protocol.

The springs already explored are summarized in table 3.1, where the concentration of activity of the spring water is also reported. The table report also the spring where the concentration was below on the minimum detectable (*b.d.m*). All the measurement reported has been conducted with the sampling protocol as indicated in the paragraph 3.1. The discussion of the results is reported in the paragraph 3.3.

The first spring investigated has been Orbo. This source was also used for a comparison between methods and measurement techniques.

3.2.2 Measurements performed in Orbo spring

Orbo is a source located on Orbo street in the Comune of Castiglione Cosentino, where there is a geological fault , the study reported in [60] has evidenced a high concentration of radon in the soil. This monitoring has been developed from 2011. The source has been monitored from August 2011 up to October 2016. The Orbo fountain does not have a precipitation box upstream or pump, then is presumable that water is directly taken from the aquifer. For all the measurement performed in Orbo site we registered air, water temperature and the water flux.

Source location	$C_{Rn}[Bq/l]$
Vurgano Schito	b.m.d.
Macchia	47 ± 4
Pertina	11 ± 1
Pompio	13 ± 1
Romana	8 ± 1
Castania	b.m.d.
Pime	b.m.d.
Pristini	140 ± 12
Orbo	63 ± 1
Mangeto	8 ± 1
Celico	b.m.d.
Settimo	12 ± 1
Parenti	11 ± 1
Qualata	24 ± 2
Versino	b.m.d.
Presila	9 ± 1
Fontana Lauro	172 ± 7

Table 3.1: Concentration activity in groundwater for various Calabria springs.

The temperature of the water and air is reported in the figure 3.1, the almost constant value, on average $(15 \pm 1)^\circ C$ of the water temperature, to respect to the wide seasonal variation of the temperature in air, indicates that there is no evidence of superficial water infiltration or effect due to external environmental temperature on the source, as expected for a deep source.

The information obtained from water flux measurements helps to know if the source is contaminated by infiltrations of superficial water or changes due to the pluvial season. If a variation of water flux is due to seasonal reason an equivalent variation of the flux should be visible. This is not the case of Orbo spring. Figure 3.2 show the water flux of the spring. The black triangle represents the mean value of the flux measured from August 2011 to April 2012 . The variation observed during three years of measurement are in the range of $[(5.5 \pm 0.5)l/min - (3.3 \pm 0.3)l/min]$. The decreasing trend of the water flux is an indication that something is changing at the origin of the source (for example the diminution of the snowing). To this variation of

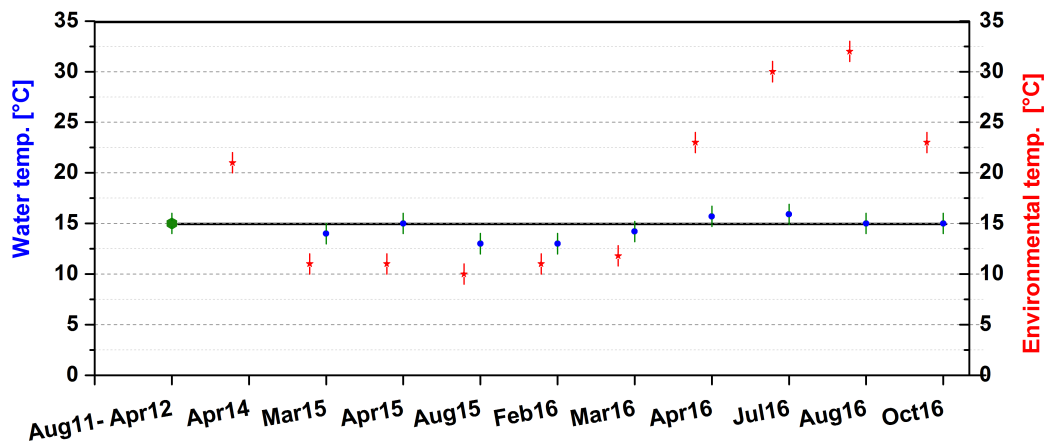


Figure 3.1: Orbo spring water temperature (dots). The green dot represent the mean value in the period [April2014–October2016]. The starts represent the environmental temperature around the fountain. The line evidences the mean value of the water temperature from April 2014 to October 2016.

the water flux is not related to a variation on the radon concentration in the spring.

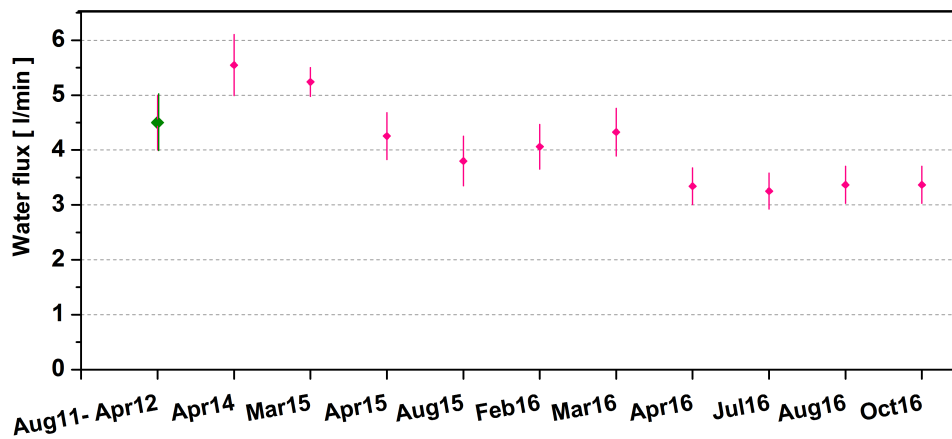


Figure 3.2: The green rhombus in the figure represent the mean value of the water flux (4.5 ± 0.5)l/min, measured from august 2011 to april 2012 .

Measure date	$C_{Rn}[Bq/l]$	Detector
August 2011 - April 2012	58 ± 8	Pylon degassing system + Lucas cell
April 2014	57 ± 6	Pylon degassing system + Lucas cell
March 2015	65 ± 2	H ₂ O Rn kit + RAD7
April 2015	58 ± 2	H ₂ O Rn kit + RAD7
August 2015	62 ± 3	H ₂ O Rn kit + RAD7
February 2016	68 ± 2	Mi.am degassing system + Lucas cell
March 2016	64 ± 3	Mi.am degassing system + Lucas cell
April 2016	61 ± 3	Mi.am degassing system + Lucas cell
July 2016	61 ± 3	Mi.am degassing system + Lucas cell
August 2016	64 ± 3	Mi.am degassing system + Lucas cell
October 2016	60 ± 2	Gamma spectrometer

Table 3.2: Radon concentration of activity measurements in Orbo spring.

All the measurements for Orbo spring are reported in Table 3.2. Each result is the combination of various samples measurements. The radon concentration of activity measured from August 2011 to April 2012 is on average 58 ± 8 Bq/l, all the measurements were performed with Lucas Cell [59].

The measurement done in April 2014 is first measurement developed for this work adopting exactly the same procedure and technique of [59]. The result is well compatible with previous measurements. The uncertainties of a single measurement was about 11%.

From March 2015 to August 2015 the RAD7 was used, for a comparison with Lucas cell detector results. The humidity correction was applied. The three measurements reported are compatible between them and with the previous ones. The uncertainties of a single measurement was about 6%. Then lower respect to the Lucas cell measurements, this is due to the larger uncertainties associated to the degassing procedure. This disadvantage, of the Pylon degassing system has been solved using a new tool for degassing: H₂O Rn kit, the measurements performed with the new tool are also included in the Table 3.2, are from February-August 2016. The measurements are in very good agreement between them and the measurements from August 2011 to April 2012. The uncertainty of the single measurement is close to 6%. The last measurement reported in the Table 3.2 was obtained with the gamma spectrometer. By this device we have observed that ²²²Rn is the only radionuclide in the sample.

A large number of measurements performed with Orbo spring allowed us to compare different detectors and degassing systems for measurements

of radon concentration in water. Various conclusions has been reached. To perform an accurate measurement with the RAD7 detector, it is necessary a considerable period of time to arrive to the best working conditions, particularly high of air humidity. The RAD7 instrumentation allows to apply a correction for measurement performed with humidity higher than 8%, but some authors report that in particular condition the correction can correspond to an over or under estimation of the concentration. Furthermore it is well understand the contribute on the uncertainty due to this correction. This detector is easy to be used, portable and offer a large range of possible measurements. The results provided are already in terms of concentration of activity. On the other hand, the Pylon scintillation detector interfaced with the Mi.am degassing system allows to assess a sample in one hour and the result is available in counts, making possible evaluating separately the contribution to the total uncertainty. Furthermore the Pylon detector is weakly dependent on the relative humidity compared with Rad7. From the comparison between detectors it is possible to conclude that the RAD7 system and the Lucas Cell + Mi.am degassing system measurements are well compatible and with the same single measurement uncertainty.

The gamma spectrometer was also used thanks to the collaboration with ARPACAL (CS). This detector is expensive from the point of view of time and cost, in fact three days are required to obtain a single result. Advantages of this technique is the higher precision and the capability to detect different radionuclide in the same sample. In a campaign of measurements the scintillation cell technique is preferable and the use of gamma spectrometry should be reserved fo the few cases in which more informations are mandatory to obtain the result. On the basis on these considerations It has been performed the measurements of Pristini, Fontana Lauro including in Table 3.1.

From the radon risk point of view, among the sources reported in the Table 3.1, only Pristini and Fontana Lauro located in Castiglione Cosentino and Pallagorio respectively, present a radon concentration higher than the limit imposed by the Italian law (100 Bq/l). Pristini is not available anymore because today is in a private area and used for irrigation only. Fontana Lauro is the most recent source tested. It is a place near to a waterfall and is one of a group of sources available to the public. This source should be tested again during different season, to quote a radon concentration mean value. It will be interesting to investigate about the reason of this high concentration of both springs and if this is the consequence of a geologic context, and it should be performed an indoor evaluation for that areas.

Orbo is a safe spring with stable concentration of activity and has been used as a reference spring for the measurements in water presented in the next chapter using the closed chamber.

3.3 Indoor radon measurements

New and restored buildings, especially public places, can need a preventive measurement of radon concentration indoor to evaluate the maximum accumulation expected. The information of this preventive measurements can helps to better design a building restoration or to inform about the maximum risk associated and the proposition of a long term measurement. Various agencies proposes guidelines [Rn measurements in new buildings. General office of Public health UFSP, Switzerland 2012, RT CTN_AGF 4/2005]. In this section will be reported a contribute to this procedures. It will be reported results of indoor measurement to estimate the laboratory background and to evaluate the maximum concentration in a public kinder garden in a mountain village of Presila, will be reported last. This measurement has been performed under the request by the local administration.

3.4 A protocol for preventive indoor measurements

As it was detailed in the Chapter 1, the main indoor radon sources are the soil, where the building is located, the sources of water spring that can enter inside the structure via domestic uses, the building materials and the outdoor radon in air. For this reason is important to collect information about geology of the zone, the available water supplies (public water network or underground water), the building uses, the heating and/or cooling system, the air tightness of the building, the number of persons and the hours per day in which the place is used . The data collected could be useful to choose the measurement site in the building and for the interpretation of the results.

The goal of the preventive measurement is to evaluate the maximum accumulation expected in the indoor place. This evaluation is performed by long term measurement. The measurement should be scheduled in the colder season when a maximum concentration is expected [61, 62]. At least one week of measurement is needed with active or passive detectors. The positioning of the detector should be where the maximum accumulation is expected and

in the places mostly frequented by people, being sure that the doors and windows are well sealed (minimizing the air flow) during the measurement. A particular attention should be reserved to dwelling in which volcanic tuff granite or in general building materials for which a high concentration is expected. If the building has a relevant source of radon, that can increase the accumulation, e.f. water supply coming from groundwater, the room should be tested carefully.

3.4.1 Indoor measurement in a Presila Kinder garden

A preliminary investigation has been performed in Calabria. In this case, the goal was to estimate the maximum radon concentration available in the structure to evaluate the potential maximum risk of the structure. The measurements have been performed using a passive short term (E-perm) detector and the scintillation cell + AB5 monitor system. Following the protocol the measurements were organized as follows.

1. Preliminary information collected:

- The building is used as a nursery.
- The structure directly resting on the floor.
- Each environment frequented by children or workers for various hours per day is equipped with large windows and doors.
- Any room was conditioned with warm or cold air.
- Each environment is frequently open for hygienic reasons, in particular: classrooms, kitchen and offices.
- There are long-term electret detectors, posed by Protection Agency (ARPACAL), in order to determine the concentration of radon gas activities, as required by law, in an interval of time sufficient to give a result expressed as an annual average of the concentration of activity of radon gas.
- The property includes a little chapel which, for reasons of cultural conservation, maintains some of the original materials (floor, stone altar, doors). The chapel is located on the ground floor and is complete with a gray stone altar of a material unknown.
- An old door and two wooden windows are a passage for external light and exchange of air.
- In the entire dwelling, except the chapel, the materials are renewed and similar between them.

2. Choose of the rooms to the detectors localization: the ambulatory, the chapel and the main hall.

- The ambulatory room was chosen because it is very similar, in terms of materials, to the classrooms attended by children and workers, the room is compact and the measurement does not disturbs the activities of the school. The small size and the total closure of the room are favorable for the accumulation gas in higher quantities, while in rooms frequented by children and workers, for reasons of service and hygiene, doors and windows are often open.
- The chapel was chosen because is located in the ground floor in contact with the floor, the presence of the original flooring and the content materials, especially the stone altar, may be a significant reason for radon gas buildup.
- In the main hall, the most used place by workers and children, was mounted a detector. In this room the measurement was performed in standard conditions i.e. opening/closing doors and with people moving inside and outside.

3. Results

Room	Detector	Indoor Rn activity concentration			Environmental parameters		
		C_{Rn} [Bq/m ³]	C_{Rn} Uncert. [Bq/m ³]	Rel. Uncert. %	Season	Temp. °C	Rel. Hum. %
1 Chapel	SST EPERM	61	11	18	Autumn	12-14	45-48
2 Chapel	SST EPERM	98	12	12	Autumn	12-14	45-48
3 Main hall	SST EPERM	0	10	–	Autumn	13-18	45-48
4 Ambulatory	SST EPERM	100	13	11	Autumn	13-17	45-60
5 Ambulatory	SST EPERM	129	13	9	Autumn	13-17	45-60
6 Ambulatory	CPRD-AB5	143,0	14,0	10	Autumn	13-17	45-60

Table 3.3: Indoor radon activity concentration results

The indoor measurements were carried out in two periods: from November 15 to November 20 and from November 26 to December 01 during 2015. For the first series of short term electret (SST E-perm) measures have been used two places, the chapel and the ambulatory room. In the second series of measurements were repeat the previous measures and also was added a SST E-perm in the main hall of the kinder garden. Additionally on the ambulatory room was located a CPRD-AB5 system. The results are summarized in

the table .

In the Table 3.3, are reported also the range of temperature and humidity for each room. In the figure 3.3, the results are compared with actual limits of Italian law for the annual mean (yellow band) and the new European Directive 59/2013, that will be law before 2018 (blue dashed line). The results are largely below the limits.

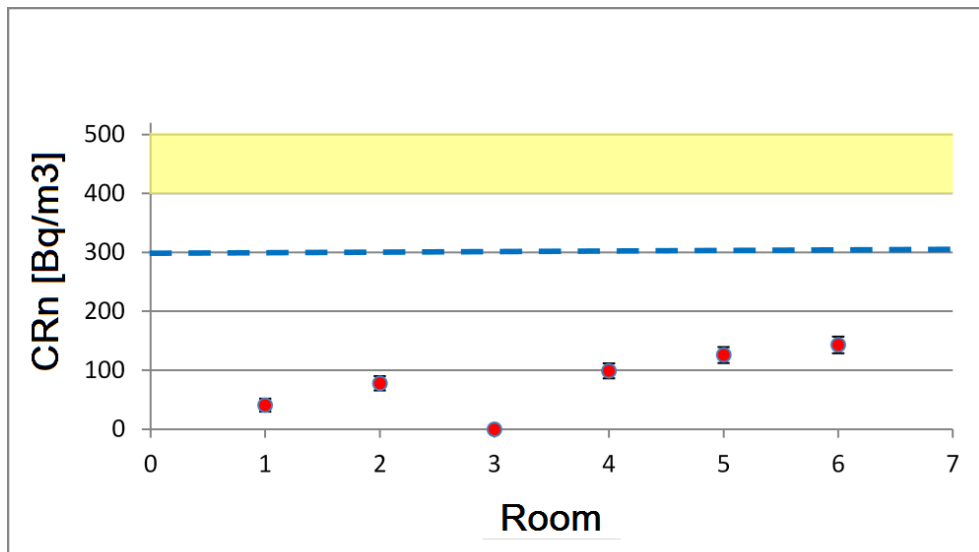


Figure 3.3: Indoor radon concentration of activity measured in various room in the Kinder garden. The numbers corresponds to the rooms indicated in Table 3.3. The yellow band represents the limit ranges of attention for the Italian law and the blue dashed line the new European limit.

3.4.2 Laboratory background

The Ionizing radiation laboratory is located on the sixth floor of the Physic's department, building 30C. It has a volume of $356 m^3$. It presents a unique door and two windows, and has three air conditioners. It is made in concrete and plywood.

Frequent measurements of indoor radon concentration of the laboratory are mandatory to quote the background for the measurements presented in

the next chapter, and because of the continuous building arriving at the laboratory for studies. During the last three years various measurements has been performed, typically one week, with different detectors: scintillation cell, RAD7, Alphaguard and electrects.

Date	Temperature	rel. Humidity	C_{Rn}	Stand. Dev
	$^{\circ}C$	%	Bq/m^3	Bq/m^3
February	15	35	54	11
March	17	51	43	11
April	22	68	35	20
July	25	59	29	8
July	26	34	31	9
December	13	75	42	11
December	12	60	51	11
April-Novembre	-	-	55	18

Table 3.4: Summary of the Ionizing Radiation Laboratory of the Physics Department indoor measurements

Table 3.4 shows the results. Information about the room temperature and relative humidity during the measurements are also reported. The last data reported in this Table was obtained with the SST E-perm detector. The other measurements were performed with the Lucas cell, except the measurement developed in March and April, which were performed with Rad7 and Alphaguard respectively. The large fluctuation of the Alphaguard result is related to the frequently use of the laboratory in these days.

In figure 3.4 are shown two measurements sets performed in the laboratory, one set in the winter and the second one in the summer. It is clearly visible the day/night effect on the measurements. The blue band in the figures shows the mean value quoted for both measurement, $(54 \pm 11)Bq/m^3$ during the winter and $(31 \pm 9)Bq/m^3$ during the summer.

Figure 3.5 shows the temporal variation of radon concentration, each point was obtained with continuous measuring with intervals of counting varying from 30 to 60 minutes. The parabolic behavior of radon concentration on the figure 3.5 confirms the well known seasonal pattern of radon activity concentration [61, 62], with a maximum during the winter and the minimum

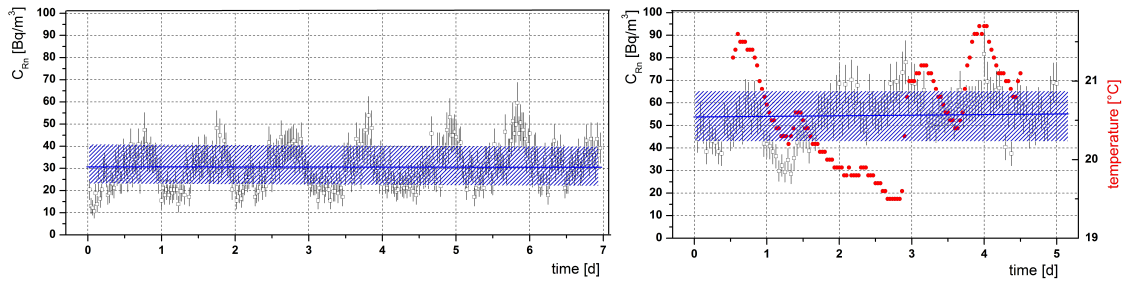


Figure 3.4: Two sets of measurements during the winter (left) and during the summer (right). Additionally on the right is included room temperature.

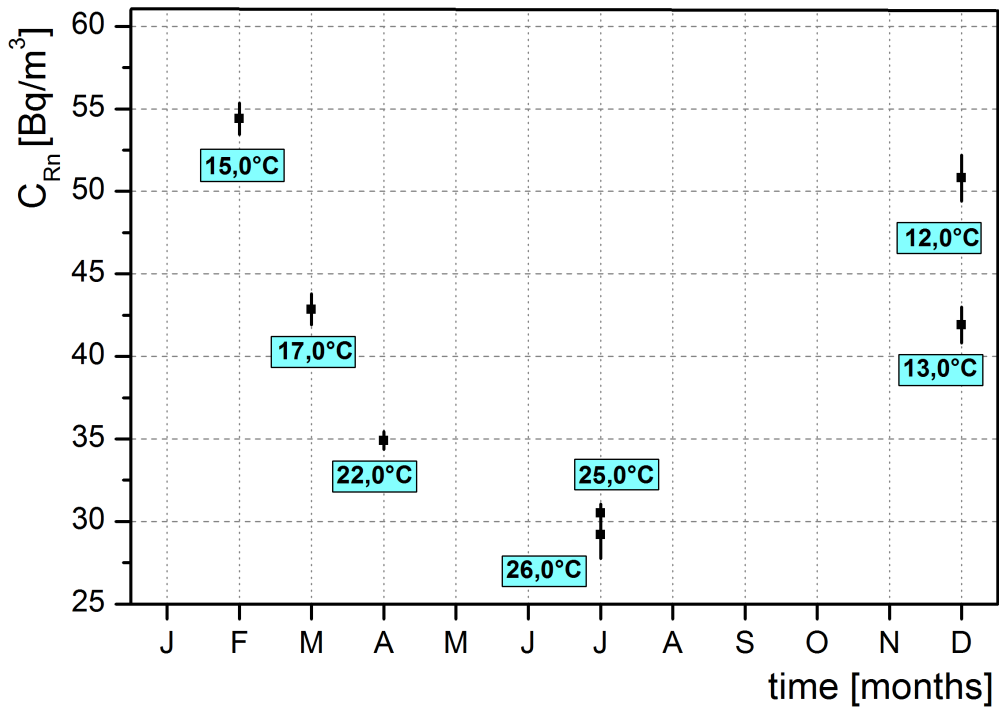


Figure 3.5: Radon concentration variation during a year in the Ionizing Radiation Laboratory. Each square represents the mean value of a set of measurements with the mean uncertainties together with the maximum value of temperature of the measurement.

during the summer. The maximum variation of the concentration during a year is about 26 Bq/m^3 , corresponding to a decreasing of 46% of the radon concentration during the summer to respect to the winter.

Chapter 4

Closed Chamber method for volcanic building materials and water assessment

4.1 Radon assessment of volcanic building materials

Radon exhalation from building material could contribute in a relevant way to the indoor radon concentration accumulation ([42] and references there in) increasing the exposure for people living or working in closed places.

Radon (^{222}Rn) exhalation from building materials is determined by the radon generation and its diffusive transport. Radon generation depends on the ^{226}Ra material content and the mechanism to exit from grain to air or water [63], while the diffusive transport depends on the porosity, permeability, grain structure and moisture content of the material [20, 64]. Various publications on experimental techniques to evaluate the contribute indoor due to exhalation from building materials are available (see for example [65, 66]).

The closed chamber method is one of the preferred approaches to assess the exhalation rate of building material[67]. This method allows to obtain accurate measurements of radon exhalation taking under control the environmental parameter, for various physical characteristics of samples: porosity, grain size, etc.

The present thesis proposes to use the closed chamber method, with two different methodology approaches, to investigate volcanic tuff samples directly collected from the North-East and North-West area of Lazio Region. The main results have been presented in two conferences (Radon in the Environment-kracov 2015 and V. Terrestrial Radionuclides in Environment International Conference on Environmental Protection- Veszprem 2016)], and now are under publication.

4.1.1 Experimental Set-up

The experimental set-up, sketched in the fig. 4.1 consist on a closed chamber interfaced with internal and/or external detectors. The chamber is made with six sheets of colorless acrylic plastic (poly methyl methacrylate PMMA), named Plexiglas G. The thermal expansion coefficient of Plexiglas G is low and a minimum thickness exhibits 100% absorbance to alpha particles. The sheets have a free area of $50 \times 50 \text{ cm}^2$ and are 1.5 cm thickness. To join them it was employed water proof silicon, additionally they were fixed with five screws at each edge to ensure the tightness of the box. Tightness has been tested filling the chamber with water; after several days no water or humidity

has been observed around the chamber and along the junctions. The volume of the chamber is 125 l. The upper sheet is movable to insert the sample and instrumentation; two swagelok connectors are positioned in this chamber face to connect an external device or to insert/extract air in a controlled way. The chamber includes the following tools: a power supply for the internal detector; a 12V fan used to mix the air inside the chamber; a shelf to support instruments (e.g. meteorological station, etc.).

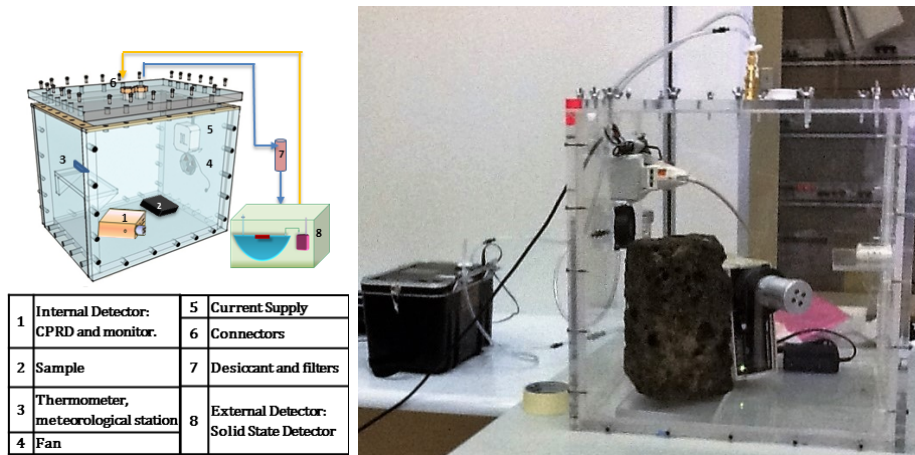


Figure 4.1: (Left) Closed chamber and its components sketch. (Right) Experiment for a comparison between Lucas cell and RAD7.

4.1.2 Detectors and samples

The measurements were performed by three types of detectors: Scintillation Lucas Cells, interfaced with a AB-5 Pylon radon monitor; a solid state alpha detector RAD7, from Durrige Company, United States; and a third detector have been used for a comparison with the Lucas cells, it is an Alphaguard. The main features of the detectors are present in the previous chapter.

The advantages of detectors are different. Alphaguard detector offer similar advantages of RAD7 detector but is less sensible to the humidity, both offer results in terms of radon activity concentration correlated with informations on temperature and humidity. A comparison between Alphaguard and Lucas Cell results is shown in fig. 4.2, the empty circles show the Alphaguard measurements performed in intervals of 10 minutes, the Lucas cell measurements performed with intervals of 70 minutes are the orange circles. The experiment was performed at laboratory conditions (21°C and a maximum relative humidity of 12 %). The curves show the well compatible results

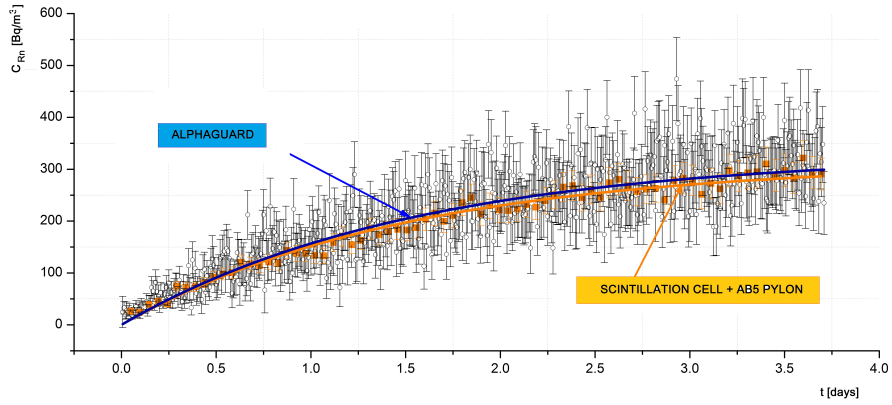


Figure 4.2: Comparison between concentration of activity measurements performed with a Pylon (orange curve) and Alphaguard (blue) detector. A curves represent the global fit results.

obtained with the global fit over the two sets of data.

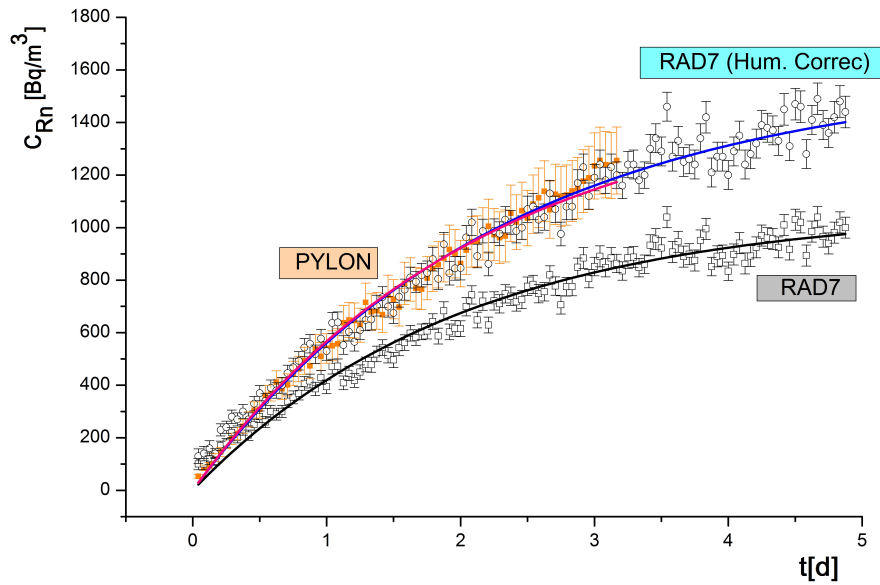


Figure 4.3: Comparison between Pylon (orange), RAD7 detector concentration of activity measurement before humidity correction (black), and RAD7 after humidity correction (blue).

The Lucas cell can be inserted in the chamber together with the sample reducing the leakage contribute due to tubes connection, it is less sensible to the humidity (see fig. 4.3) and provides results in terms of counting allowing separate studies of the contribute to the total uncertainty, a disadvantage of the detector inside the chamber is that it reduce the net volume of the chamber.

RAD7 detector offer the opportunity of a contemporaneous measurement of the temperature and humidity during the accumulation and presents results already in terms of concentration of activity, the large susceptibility to the air humidity requires an important correction. Figure 4.3, shows a comparison between Lucas cell and RAD7 detector, without and with humidity correction. Durriged offer a software, but it remains unclear which are the limits of applicability of correction and the contribute in terms of uncertainties. Figure 4.3 shows the concentration of activity as a function of the time in the accumulation chamber, with intervals of measurements of one hour and with experimental conditions of large humidity (40% to 90%). The empty black squares are RAD7 results obtained without humidity correction, the empty black squares shows the RAD7 results after humidity correction and the orange circles are measurements performed with Lucas cells, is clearly visible the effect of humidity on RAD7 measurements. After correction the measurement are well compatible.

For the purposes of this work was chosen as the reference detector the scintillation Lucas cell.

The choice of the investigated materials is related to the large use of tuff as building material in the central part of Italy, in fig.4.4 is shown an example where is clearly visible (left) part of a building completely realized with tuff blocks and (right) a detail of a tuff brick of the wall.

Tuff building materials are soft rocks made of volcanic ash ejected during a volcanic eruption. Tuff construction materials are characterized by a high porosity, a high water absorption, low conductivity [68] and a wide disparity in grain sizes, ranging from fine ash ($< 1/16$ mm) to lapilli-sized fragments (< 64 mm) [69]. Various publication reported results on tuff exhalation rate (see for example [70, 65, 71, 72]) showing the large range of variability of the results related to the large variety of tuff materials due to the different chemical and physical properties between samples. In particular [70] presented results for Italian tuff ranging from $0,041 \pm 0,004$ and $0,17 \pm 0,02$ Bq kg⁻¹ h⁻¹. For this reason a dedicated set of measurements is needed for different



Figure 4.4: A house of Lazio Region using tuff building materials for external walling (left) and a particular of a tuff brick (right).

caves of extraction.

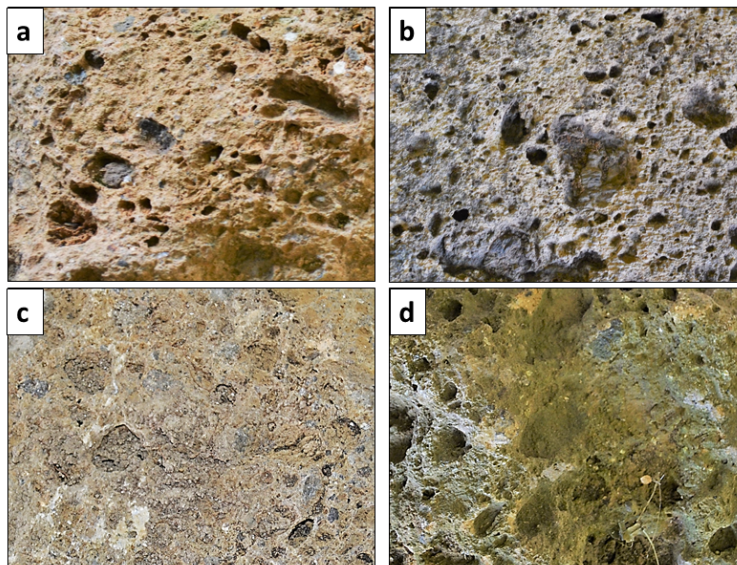


Figure 4.5: Tuff building materials samples analyzed. Is clearly visible the different porosity of the samples, the different colors and the different number of inclusions between samples.

Four tuff samples were selected for this analysis and shown in fig.4.5. The sample *a* came from Cervetri area, closed to the North-West Lazio Region,

the others three samples are from the Torrita Tiberina area in the North-East of Lazio Region of Italy (*Media valle del Tevere*), where a copious amounts and a large variety of these were building materials are available and often used because economic, light material and aesthetically pleasing, for details on the stratigraphy and geological evaluation of the areas investigated see for example [73].

The samples were chosen intentionally different in terms of composition, color and density. Tuff samples coming from Torrita Tiberina were taken directly from the materials used for buildings.

All the samples were weighted and dried during 48 hours at 100°C before the analysis. To dry the samples is important to reduce the dependence of the results on the water content.

Figure 4.6 shows the comparison of the radon concentration of activity for the same tuff sample; before any treatment (purple line), humidify sample (orange line) and after drying (green line). It is visible a different rapidity of accumulation before and after drying in the same material in the closed chamber for all three different treatments. As expected the sample with higher content of water shows the lower exhalation rate. Moreover the difference of accumulation rapidity, between the sample like it was when it arrived to the laboratory and after immersion in water, is not so high. It confirms that is important to dry the samples before any exhalation rate measurement.

4.1.3 Experimental procedure

The closed chamber method consists in enclosing the tuff building material inside the hermetical chamber, radon is exhaled to the free volume of the chamber, and accumulated in time. Depending on the radon content and other characteristic of the sample, accumulated radon reach an equilibrium state between exhaled and decayed nuclide after few hours or several days. The equilibrium state between the exhaled radon and the natural decay can be modified by radon back diffusion toward the sample and/or a radon lost due to leakage of the chamber. The back diffusion term can be considered negligible if the free air volume of the chamber is significantly larger than the sample volume [67]. Our chamber is big enough, compared to the samples volume, to avoid this effect.

When the material has a well defined surface it is convenient to express the exhalation rate in terms of *surface exhalation rate*, which is defined as

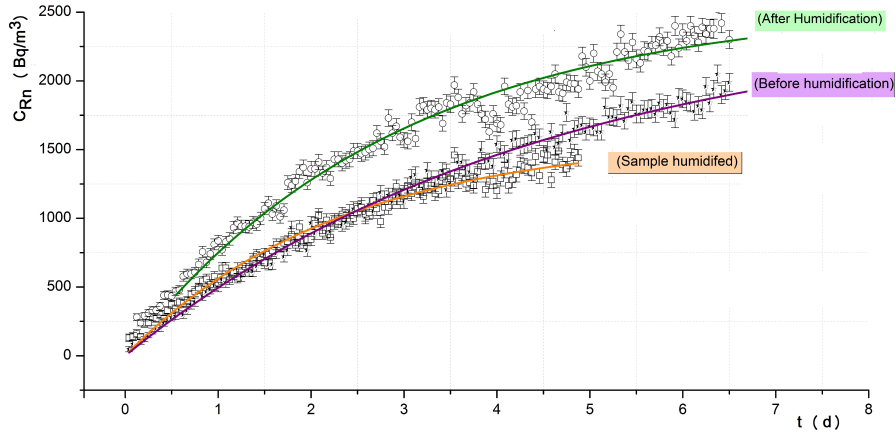


Figure 4.6: Tuff building materials samples measured before and after drying. The purple curve shows the fit results obtained with the sample like it was in the building, the orange curve shows the fit result with the humidify sample and the green curve shows the fit result of the same sample after 48 hours drying at 100°C.

the number of radon atoms leaving unit surface area of the material per time unit ($Bq m^{-2} s^{-1}$), in the case of powders or not well-defined surfaces it is preferable to express it in terms of *mass exhalation rate* or *specific exhalation*, which is defined as the number of radon atoms emitted in mass and time unit ($Bq kg^{-1} s^{-1}$).

Due to the large irregularity of the tuff samples, results are presented in terms of mass exhalation rate.

4.1.4 Radon exhalation rate

When a material is enclosed in the chamber, due to the continuous exhalation of the sample, radon is accumulated and the radon activity concentration $C(t)$ growth in time until it reaches the equilibrium state. This process can be described by the equation

$$\frac{dC(t)}{dt} = -\lambda_{eff}C + \frac{E_0 m}{V_{air}} + \lambda_l C_{Bg} \quad (4.1)$$

where

$$\lambda_{eff} = \lambda_{Rn} + \lambda_l + \lambda_b$$

The first term in (4.1) indicates that radon accumulation is characterized by a effective decay rate λ_{eff} that includes the radon decay constant λ_{Rn} , the chamber leakage rate λ_l and the back diffusion rate λ_b . The second term depends on the mass radon exhalation rate contribution E_0 . m is the mass of the sample and V_{air} the net volume of the chamber. The last term includes the radon exchange between the chamber and the laboratory due to the leakage of the chamber characterized by λ_l , C_{Bg} is the radon concentration background in air.

The initial exhalation rate E_0 is the radon exhalation rate when C is compatible with the chamber background. The exhalation rate E_0 decreases with a linear low to the increasing of the concentration in the chamber, due to the back diffusion effect:

$$E = E_0 - \frac{DV}{A} \quad (4.2)$$

The solution of equation (4.1) with the initial conditions: $C(t) = C_i$ at $t = 0$, where C_i is the initial radon concentration (it can vary depending on the cleaning of the closed chamber).

$$C(t) = C_i e^{-\lambda_{eff}t} + \frac{Em}{V_{air}\lambda_{eff}} (1 - e^{-\lambda_{eff}t}) + \frac{\lambda_l C_{Bg}}{\lambda_{eff}} (1 - e^{-\lambda_{eff}t}) \quad (4.3)$$

From 4.3, the radon concentration at equilibrium state, is:

$$C(\infty) \cong \frac{E_0 m}{V_{air}\lambda_{eff}} + \frac{\lambda_l C_{Bg}}{\lambda_{eff}} \quad (4.4)$$

and the mass exhalation rate can be obtained,

$$E_0 = (C_\infty \lambda_{eff} - \lambda_l C_{Bg}) \frac{V_{air}}{m} \quad (4.5)$$

The parameter $C(\infty)$ and λ_l can be extracted with a global fit with the function (4.3), assuming λ_b is negligible.

The differential to the equation 4.3 when the time tends to zero, allows to obtain the initial slope of the radon growing curve M_g .

$$\frac{dC(t)}{dt_{(t \rightarrow 0)}} = M_g = \frac{Em}{V_{air}} + \lambda_l C_{Bg} - \lambda_{eff} C_i \quad (4.6)$$

M_g represents the rapidity of the radon accumulation inside the closed chamber that is related to the radon exhalation of the material. With this method can be assumed that the initial growing slope M_g is independent from the back diffusion effect and from initial radon exhalation.

Knowing the growing slope M_g , E_0 can be extracted.

$$E_0 = (M_g - \lambda_l C_{Bg} + \lambda_{eff} C_i) \frac{V_{air}}{m} \quad (4.7)$$

This method has the advantage of allowing fast measurements to respect to the previous method described and it is not affected by the back diffusion effect. The main disadvantages of the method are related to the relative poor statistic corresponding to fluctuation due to the low concentration at the beginning of the measurement.

4.1.5 Chamber leakage rate

An outflow and inflow air can occur through the lid junctions. Leakage rate is clearly an important parameter to characterize the chamber performance and to estimate the exhalation rate of materials with a closed chamber method. The theoretical decreasing of the concentration is

$$C_{th} = C_0 e^{-\lambda_{Rn} t} \quad (4.8)$$

Assuming the chamber only filled with air containing radon, at the chamber closing the radon concentration is C_0 . If the differential is applied in the limit when $t \rightarrow 0$, the initial slope of the theoretical decay curve is

$$\frac{dC_{th}}{dt_{(t \rightarrow 0)}} = M_{th} = -\lambda_{Rn} C_0 \quad (4.9)$$

If there is a chamber leakage, the rate of decreasing is faster than λ_{Rn} , due to the contribution of chamber leakage rate λ_l . In absence of the sample does not exist the back diffusion contribute, then the effective rate is $\lambda_{eff} = \lambda_{Rn} + \lambda_l$.

The decreasing of the experimental radon concentration C_{ex} is

$$C_{ex} = C_0 e^{-\lambda_{eff} t} + \frac{\lambda_l}{\lambda_{eff}} C_{Bg} - \frac{\lambda_l}{\lambda_{eff}} C_{Bg} e^{-\lambda_{eff} t} \quad (4.10)$$

where C_0 is initial radon concentration. Applying the differential at the limit when $t \rightarrow 0$, the initial slope of the experimental decay curve yields:

$$\frac{dC_{ex}}{dt(t \rightarrow 0)} = M_{ex} = -\lambda_{eff} C_0 + \lambda_l C_{Bg} \quad (4.11)$$

A method to determine the chamber leakage rate is to compare the initial slopes of the radon decay curve M_{th} and M_{ex} . The difference between theoretical and experimental points out the chamber radon lost rate λ_l due to the leakage

$$M_{th} - M_{ex} = \lambda_l (C_0 - C_{Bg}) \quad (4.12)$$

$$\lambda_l = \frac{M_{th} - M_{ex}}{C_0 - C_{Bg}} \quad (4.13)$$

An alternative to the linear fit to extract λ_l parameter is a global fit with 4.10 assuming free parameters λ_l and C_0 .

4.1.6 Back diffusion rate

If the radon activity concentration in the closed chamber is higher compared to the radon activity concentration in the pore of the sample, a certain amount of radon back to the sample following the Fick's law. This effect is called back diffusion. The rate of back diffusion λ_b , can be obtained replacing the equation 4.6 in the equation (4.4).

$$\lambda_b = \frac{1}{C_\infty} \left(\frac{Em}{V_{air} \lambda_{eff}} + \frac{\lambda_l C_{Bg}}{\lambda_{eff}} \right) - \lambda_{Rn} - \lambda_l \quad (4.14)$$

$$\lambda_b = \left(\frac{M_g}{C_\infty - C_i} \right) - \lambda_{Rn} - \lambda_l \quad (4.15)$$

As expected, in various tests conducted we found a back diffusion rate compatible with zero within the error.

4.1.7 Background

The evaluate of the chamber background C_{Bg} , is needed to obtain λ_l and E with the linear fit. Various authors (see for example [66]) used the concentration measured in the laboratory where the chamber is installed. This procedure, as it was explained in 3.5.2, does not take into account the wide variation between seasons and a large day/night fluctuation of the concentration measured. Furthermore depending on the temperature excursions the concentration of the laboratory can vary 20-30 % .

Figure 4.7 and 4.8 display two independent measurements done in the laboratory and inside the empty closed chamber during at least 7 days. In figure 4.7 is clearly visible the wide fluctuation between day and night measurements, in figure 4.8 radon concentration shows smaller fluctuation respect to the laboratory measurement.

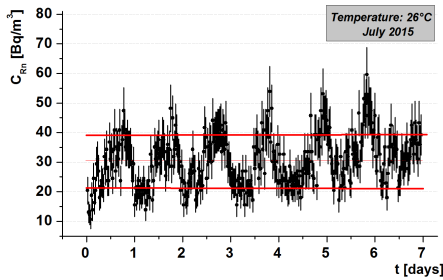


Figure 4.7: Laboratory concentration measurements.

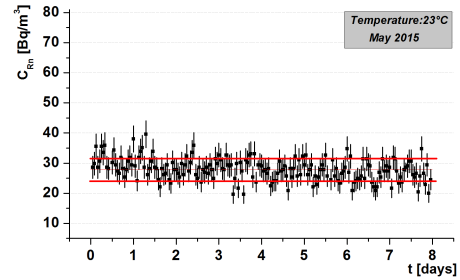


Figure 4.8: Concentration measurement inside the chamber.

Moreover, the radon concentration in the air of the laboratory is the same of the empty closed chamber (if no cleaning process is applied to the chamber), however the mean value of radon activity in the laboratory varies between $(29 \pm 8)Bq/m^3$ to $(55 \pm 11)Bq/m^3$ corresponding to a temperature variation from $12^\circ C$ to $26^\circ C$. The mean value of radon activity concentration inside the closed chamber is $(29 \pm 1)Bq/m^3$ with a stable temperature close to $21^\circ C$.

However, a chamber background measurement has been repeated before each measurement to verify that its stability in fact residual fragments of powder coming from samples analyzed can modified the background of the chamber or in laboratory.

For this reason we choose to use the mean radon concentration value obtained in the closed chamber to estimate the background of the exhalation

measurement to respect to what is typically done to reduce significantly the contribute to the total uncertainties due to this parameter.

4.1.8 Results and discussion

Chamber leakage

To quantify the leakage rate λ_l , several tests were conducted with different detectors.

A tuff sample was inserted inside the chamber, the chamber was well sealed and after a couple of weeks the sample was quickly removed and then the chamber was resealed. A fraction of the gas previously accumulated still remains in the chamber and it decays following the radon exponential decay law 4.8, characterize by $\lambda_{Rn} = 0,007554[h^{-1}]$. After the sample removal, the accumulated radon concentration is the initial radon concentration C_0 in the chamber in equation 4.13.

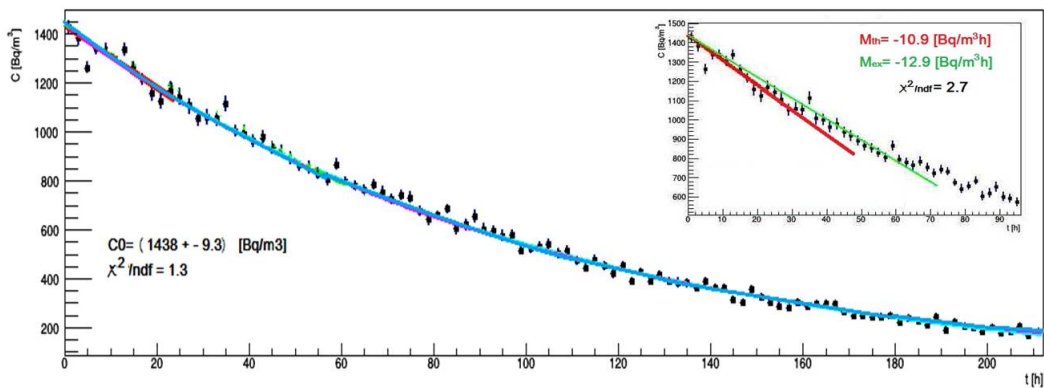


Figure 4.9: Radon concentration of activity measured in the empty chamber . The blue line shows results of the global fit. The green line and the red line (magnified in the insert) represent the experimental slope obtained with a linear fit and the theoretical expectation respectively.

Figure 4.9 reports an example of leakage measurement, the blue curve shows the global fit results, the green and red curves show the theoretical and the experimental slope. This measurement is one of the results reported in the Table 4.1 (first line).

Table (4.1) reports results from five test applying the two methods mentioned in the previous section. The three samples b , c and d from Torrita Tiberina have been used. The table shows also the air change rate ACR obtained. All the results are compatible within the errors.

Detector and Sample	Linear fit				Global fit			
	λ_l [h^{-1}]	Uncer. %	$\chi^2/ndof$	ACR [l/h]	λ_l [h^{-1}]	Uncer. %	$\chi^2/ndof$	ACR [l/h]
Rad7-b	0.0015	31	2.7	0.172	0.0019	11	1.1	0.220
Scintillation cell-b	0.0024	11	3.9	0.289	0.0026	2	1.8	0.307
Scintillation cell-b	0.0021	15	3.8	0.248	0.0024	2	1.9	0.287
Scintillation cell-c	0.0035	10	2.2	0.418	0.0037	4	1.6	0.444
Scintillation cell-d	0.0031	9	3.1	0.37				

Table 4.1: Leakage rate results for different detector and samples, the reduced χ^2 and ACR obtained with a linear and a global fit.

In particular, the fit obtained with the sample b and the scintillation cell are in very good agreement for both methods. They are also compatible with the test performed with RAD7 detector. In this last case, due to the data fluctuation, the uncertainty is higher.

The last two results reported in the Table (4.1), obtained with samples c and d with the same detector, confirm the compatibility of the two methods. With the sample d has been impossible to obtain the leakage with the global fit, due to the large fluctuation of the distribution after 2 days of measurements, the reason is not well understood. Higher leakage to respect to the results obtained with sample b , is due to the upgrade of the closed chamber for radon concentration measurements in water. The problem was resolved better sealing the chamber (cf. next section).

The global fit is a more accurate method even if it requires days of measurement and, is preferably respect to the method proposed by [65, 66]).

Mass exhalation rate

The sample a was used to compare methods and test the experimental procedure. The results on Table (4.2) indicates clearly the agreement between the methods used to estimate the radon exhalation rate of building materials. For all the measurements on the table, the counting intervals are one hour except for the last result in the table where the intervals was two hours.

A set of 5 measurements were carried out with the sample b . The results are well compatible between them. Figure 4.10 shows an example of fitting of the sample b . The blue curve is the result of the global fit, the green and

Detector	Linear fit			Global fit		
	E_0 [Bq/kg h]	Uncer. %	$\chi^2/ndof$	E_0 [Bq/kg h]	Uncer. %	$\chi^2/ndof$
Alphaguard	0.40	5	0.5	0.39	3	0.7
Scintillation cell	0.35	6	1.3	0.35	5	0.8
Scintillation cell	0.36	3	0.9	0.35	3	0.4
Scintillation cell	0.31	14	1.1	0.37	9	0.4

Table 4.2: Mass exhalation rate results for sample *a*.

the red lines show the result of the linear fit performed on the first 24 hours data and the theoretical expectation respectively.

The Table (4.3) summarize the results for the four samples. The exhalation can be accurately evaluated with both methods. The equilibrium state of radon concentration is reached after a long period of time, for example the test shown in the figure 4.10 a period more than 400 hours has been necessary to reach the equilibrium state. Instead the time to obtain the initial slope of the accumulation curve is about 24 hours.

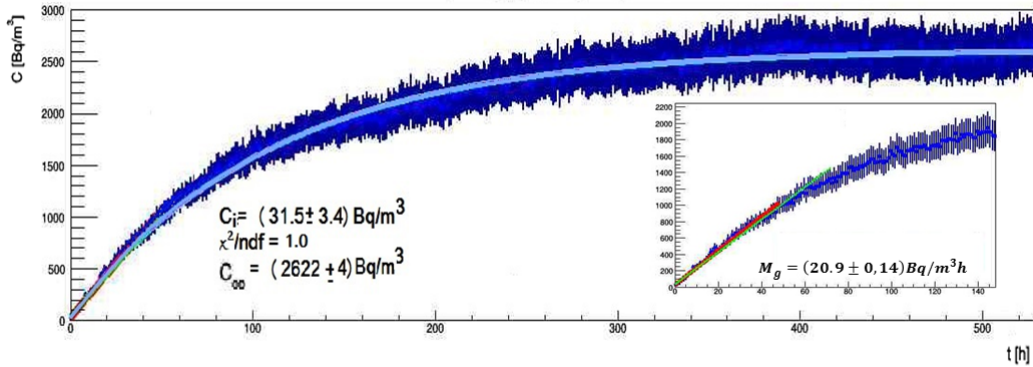


Figure 4.10: Radon concentration activity as function of time, accumulated in the closed chamber using the sample *b*. The blue curve represents the result of the global fit. The green line is the result of linear fit to the experimental data and the red line is the theoretical slope. The insert magnifies the initial accumulation period.

The large difference between results, presented in Table (4.3), was expected, already reported in [70] and confirmed by this thesis. It is certainly due to a different content of radium in the samples but also the texture, porosity and grain size contribute significantly of the exhalation. For this reason are in program analysis to evaluate the radium content of the materials and

Sample	Linear fit		Global fit	
	E_0 [Bq/kg h]	Uncer. %	E_0 [Bq/kg h]	Uncer. %
a	0.36	2.0	0.37	1.9
b	0.46	1.0	0.51	0.9
c	0.23	2.1	0.24	1.1
d	0.58	2.0	0.63	1.9

Table 4.3: Mass exhalation rate results of the four samples assessed.

other tests with the samples analyzed. Since these tests are destructive they have been postponed to the end of the measurements.

4.2 An alternative method for radon concentration measurement in water using a closed chamber

The closed chamber presented in the section 4.1 and used for the exhalation rate measurements was modified to assess water samples in terms of radon activity concentration from springs. This method will be compared with the measurements reported in the chapter 3 for the Orbo source.

4.2.1 Experimental procedure

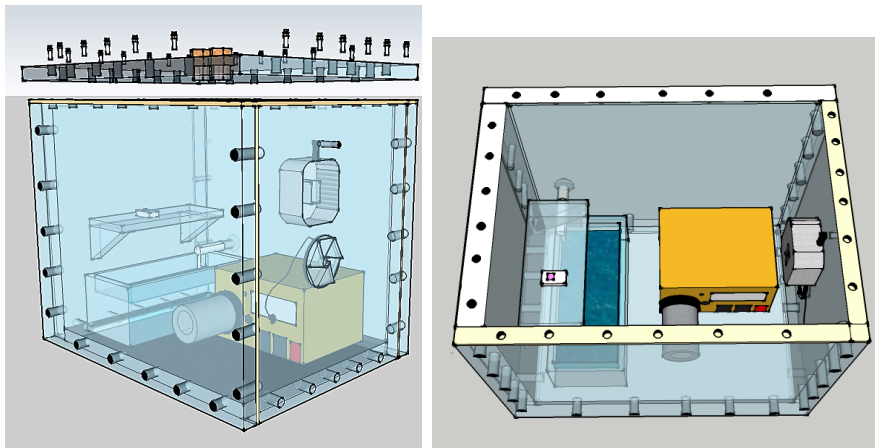


Figure 4.11: (Left) Closed chamber updated to develop water radon measurements. The figure shows the experimental set up before of inserting the water sample, once the detector have been set on. (Right) Internal closed chamber sketch. The figure shows the internal panorama after the water inserting (in real conditions the system should be hermetically closed)

The experiment consist in enclosing a know volume of water together with a radon detector inside the closed chamber and measuring the concentration growing in the chamber. The chamber upgrade consist on adding an entrance on the lateral wall of the chamber were was inserted a gas tight tap, a tube connect the tap to the bottom of the glass container to reduce the turbulence created when water is poured inside. The test samples used are from a spring largely monitored, Orbo spring. The mean concentration of Orbo water is 63 ± 1 Bq/l.

4.2.2 Method

Since the sample of water has been inserted in the box inside the chamber keeping the turbulence as low as possible, radon is naturally transported (mainly by diffusion) from water to air through the contact surface. The physical problem of transport of radon from water to air can be reduced to one-dimensional diffusion. Assuming radon uniformly distributed in any horizontal plane, the equations 4.16 and 4.17 represent the radon diffusion process (see fig. 4.12) in the vertical coordinate $z \in (0, L)$.

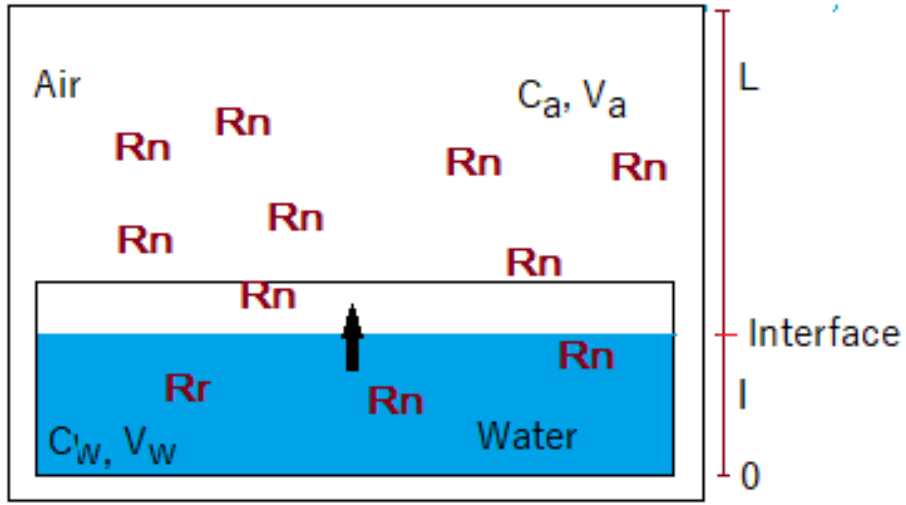


Figure 4.12: Sketch of the diffusion process.

$$\frac{\partial C_w}{\partial t} = D_w \frac{\partial^2 C_w}{\partial z^2} + \lambda_{Rn} C_w, \quad z \in (0, l) \quad (4.16)$$

$$\frac{\partial C_a}{\partial t} = D_a \frac{\partial^2 C_a}{\partial z^2} + \lambda_{Rn} C_a, \quad z \in (l, L) \quad (4.17)$$

Where, C_w is the radon activity concentration in water and C_a radon activity concentration in air, considered as functions of the vertical coordinate z , the diffusion coefficients of both phases, water and air are D_w and D_a and λ_{Rn} is the decay rate constant of radon.

At the common interface (water-air), the continuity of the radon flux denoted as F , can not be evaluated. It must be replaced by a discontinuity [74] condition given by 4.18. F is the radon flux defined as the number of atoms that cross a unit of area per time unit, F is measured in Bq/m^2s (see eq. 4.18).

$$F(t) = \beta [C_w(t) - \alpha C_a(t)] \quad (4.18)$$

α and β are two constants characteristics of radon. α is the Ostwald coefficient, it gives the orientation of the radon flux, its value depends on the temperature [75], varying from 0.525 at 0°C to 0.226 at 25°C, α can be obtained as the ratio between the radon concentration in water at the equilibrium state, C_w^{eq} , and the radon concentration in air at equilibrium state C_a^{eq} , $\alpha = C_w^{eq}/C_a^{eq}$. β has the dimension of a velocity [m/s] and is the radon velocity transfer between air to water.

The total radon activity A inside the chamber is the sum of the activity of radon in air plus the activity of radon in water.

$$A_t = (C_a^{eq}V_a + C_w^{eq}V_w) e^{t_{eq}\lambda_{eff}} = (C_a^{eq}V_a + \alpha C_a^{eq}V_w) e^{t_{eq}\lambda_{eff}} \quad (4.19)$$

$$(4.20)$$

Where, V_a and V_w are the volume of water and air respectively. λ_{eff} takes into account the spontaneous radon decay and the chamber leakage.

From equation 4.19, the radon concentration in water before the transfer can be determinate [76].

$$C_w = \left(C_a^{eq*} \frac{V_a}{V_w} + \alpha C_a^{eq*} \right) e^{t\lambda_{eff}} \quad (4.21)$$

Where C_a^{eq*} is the experimental value of the radon concentration in air at equilibrium state corrected subtracting the radon concentration background of the chamber C_{Bg} . C_w is the value of the radon concentration of water at the initial time, when the water sample was inserted in the chamber. To obtain the radon concentration of water at the time of sampling, the correction for the time should be applied.

4.2.3 Results and discussion

Three tests with Orbo spring water has been performed. Figure 4.13 shows the first test of concentration of activity in the chamber as a function of the time. In the figure is visible the fast increasing of radon concentration in air until the equilibrium time. After the equilibrium the exponential decreasing

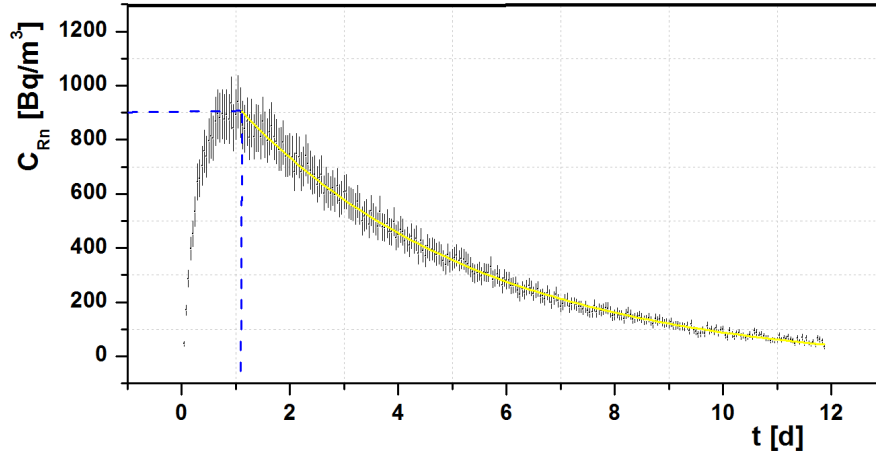


Figure 4.13: Radon accumulation and Radon decay curve.

of the radon concentration has been used to quantify the leakage rate of the chamber. Applying the global fit, as it was described in in the section 4.1.5, the leakage rate obtained is $0.0023 \pm 4 \% h^{-1}$ ($\chi^2/ndof = 1.4$).

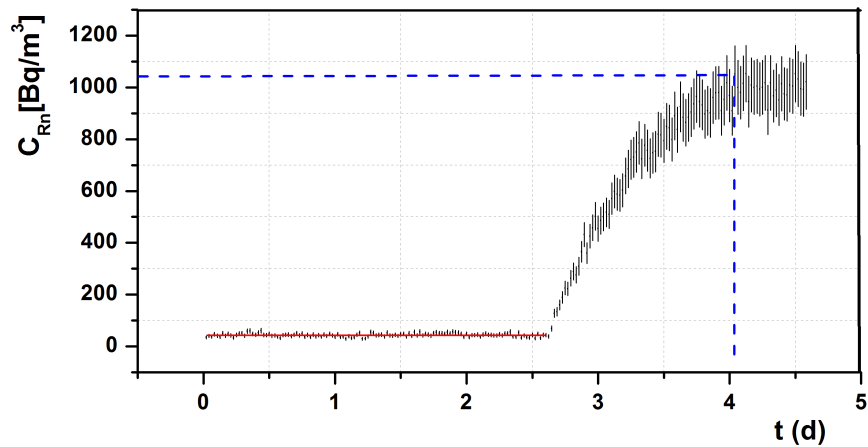


Figure 4.14: Background of the chamber and accumulation curve.

The second sample has been used also to measure the background of the chamber, the figure 4.14 shows the concentration as function of the time, for two periods, before and after the insertion of the water in the chamber. The first part was used to evaluate the background of the chamber during the

period of the test. The result of the chamber background is 44 ± 1 Bq/l. The volume of the three samples was 2 l for the first two test and 3.5 l for the last one, and the net volume of the chamber was 110.0 l and $108.5 \text{ l} \pm 1\%$.

Table 4.4 includes the parameters needed in equation (4.21) to extract the radon concentration from the three water samples.

Experiment	1	2	3	
Date	Nov-15	Jul-16	Nov-16	
C_a^{eq}	900 ± 54	926 ± 46	1050 ± 42	Bq/m^3
α	0.25	0.25	0.25	
t	20	18	31	h
C_{Bg}	$44 \pm 2\%$	$44 \pm 2\%$	$44 \pm 2\%$	Bq/m^3
λ_l	$0.0023 \pm 4\%$	$0.0023 \pm 4\%$	$0.0023 \pm 4\%$	h^{-1}

Table 4.4: Parameters used to calculate the initial radon concentration in water C_w , with the equation (4.21).

The results are reported in Table 4.5, they are in good agreement among them and they are consistent with the Orbo concentration measured with the emanometry technique (63 ± 1 Bq/l) and with gamma spectrometry (60 ± 2 Bq/l), reported in Table 3.2.

The results obtained with our closed chamber has been recently obtained and should be considered as preliminary results. They should be corroborated with various other tests, as for example: studies of the effect of the turbulence produced during insertion of the water sample in the chamber, the dependences on the water temperature, the dependence on the salinity of the water and on the humidity of the chamber, etc.

The proposed method is an original alternative to the standard methods used. It does not depend on the degassing efficiency and can be used with conventional detector for measurements in air.

Experiment	C_w	Relative error
	Bq/l	%
1	58 ± 3	5
2	58 ± 3	5
3	62 ± 5	8

Table 4.5: Radon concentration of the Orbo spring obtained with the closed chamber method.

Chapter 5

A program to transfer the knowledge to Ecuador

My PhD has been supported by SENESCYT (*Secretaría de Educación Superior, Ciencia, Tecnología e Innovación of Ecuador*), with also the goal of learning and later to transfer techniques and methods for radon concentration of activity measurements in air, water and for assessment of exhalation rates of building materials. //

In this final chapter will be exposed the main lines of a pilot project dedicated to the design of an extended campaign of ^{222}Rn concentration activity measurement in water, building material and indoor places, taking in account the wide variety of environments where radon can be found and the influence of the peculiar climatological and geological conditions of the country.

5.1 Main features of Ecuador

Ecuador is 283,561 km^2 in size including the Galapagos Islands, it is located on the west by the Pacific Ocean, and has 2,237 km of coastline (see fig. 5.1). It has 2237 km of land boundaries, with Colombia in the north (708 km border) and Peru in the east and south (1,529 km border). In 2014 the population was 15.98 million people. Ecuador is divided into three continental regions, Costa (Coast), Andes or Sierra (Mountains), and Amazony (East) and a insular region the Galapagos Islands (officially Archipiélago de Colón).



Figure 5.1: Ecuador map. The four regions are showed, Galapagos Islands in blue, Coast region in light yellow, Sierra or Andes region is in dark yellow and the Amazony is in green. Map taken from [77].

Each region has its own complex and diversity geology, climatic and anthropological characteristics. For example, Galapagos Islands are a group of volcanic islands formed by a volcanic hotspot located in the East Pacific Ocean. Galapagos are thought to be the product of a mantle plume. Mantle plumes are columns of hot rock, roughly 100 km in diameter, that rise from deep within the Earth. Two distinct types of volcanoes occur in the Galapagos. The difference between these two volcanic morphologies appears to

be due to the difference in lithospheric thickness. Climate on the Galápagos range from 21 to 28°C during the year. The warmer months experience no precipitation, whereas the cooler months of January through April have some fog and drizzle.

About the Coast region, it is estimated that 98% of the native forest of coastal Ecuador has been eliminated in favor of cattle ranching and other agricultural production, including banana, cacao and coffee plantations. The Costa is influenced primarily by proximity to warm or cool ocean currents. The mean diurnal annual temperature in the Coast region is 35°C , and the mean nocturnal annual temperature is 19°C . Although seasonal changes in temperature are not pronounced, the hottest period occurs during the rainy season, especially from February to April.

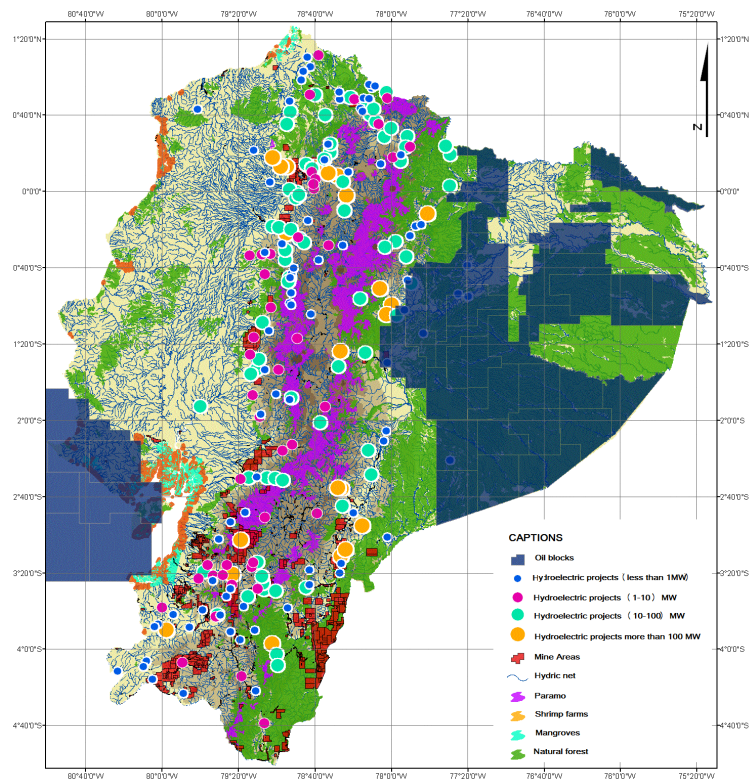


Figure 5.2: Ecuador map where is shown mine and oil projects, also the natural forests, shrimp farms and mangroves. Map adapted from reference [78].

Amazony is one of the world's last high biodiversity wilderness areas.



Figure 5.3: The volcanic zone of continental Ecuador is located in the Sierra region where are identify 29 volcanoes. The main volcanoes are: Chimborazo (6,267 m a.s.l) inactive volcano, the furthest point from the Earth's center. Cotopaxi (5,897 m a.s.l) the second highest active volcano in the world. Illiniza (5,248 m a.s.l), Tungurahua (5,023 m a.s.l) active volcano, Quilotoa (5,070 m a.s.l) inactive volcano and Pichincha (4,784 m a.s.l) active volcano. Figure taken from [79] .

Much of the Amazony is tropical moist broadleaf forest (jungle), with strikingly different upland rainforest with steep, rugged ridges, cascading streams and lowland rainforest [80, 81]. The east of the region is home to a large

number of Ecuador ethnics groups including Taromenane and Tagaeiri tribes, which are no contacted families [82]. The oil fields are located in the Amazon basin and a few on the ocean and and coast region (see the dark blue blocks in the fig.5.2). The main gold, silver and cooper mines are located on the south/east of the region (see the red squares on fig.5.2), part of them are open sky mines. Temperatures on the Amazony average from $25^{\circ}C$ in the western parts of this region, and $28^{\circ}C$ in the east. The jungle cover the eastern side of the lowland, it register high levels of rainfall sometimes exceeding 5,000 millimeters per year (tree times more than Roma).

Sierra presents volcanoes and mountain peaks that have snow during all the year (see figure 5.3). Part of the mine area is located on the south of this region being the most controversial the projects "Rio Blanco" and "Loma Larga" located in Azuay, because they are gold and silver deposits located in the origin of the main water supply of the province, and the older mines are located in the south of this region, specially in Loja (see the red squares on fig.5.2). Climate in the Sierra is divided into levels based on altitude. The tropical level from 400 to 2000 m a.s.l has temperatures ranging from (20 to $25^{\circ}C$) and heavy precipitation. The subtropical level from 1800 to 2500 m a.s.l temperatures from (12 to $25^{\circ}C$) and moderate precipitation. The level from 2500 to 3200 m a.s.l has an annual temperature range of (10 to $15^{\circ}C$) and an annual rainfall of 1,000 millimeters. Above 4650 m a.s.l is the frozen level, where peaks are constantly capped with snow and ice, and temperatures range from below 0 to $3^{\circ}C$. Precipitation frequently is in the form of snow, fog, and rain.

5.2 Objectives and justification

Ecuador is an extended and important Country, with a wide variety of political, economical and geological aspects. To design an extended campaign of measurements of ^{222}Rn concentration activity in water, building materials and indoor places, is not simple. A dedicated pilot project, in limited pilot areas, is needed for an efficient programming of a campaign extended to all the Country. A correct choise of the pilot areas is mandatory to well decide times, instrumantations and procedures. The objectives of a three years pilot project are:

1. **Radio protection:** to evaluate the radon risk due to building materials, springs water and indoor air exposition of Ecuadorian population.

2. **International databanks:** to contribute to the worldwide monitoring databases with new data collected in Ecuador.
3. **Scientific research:** The Ecuador climate, makes this country an ideal sky open laboratory to study the dependences of radon concentration of activity from climatic parameters and environmental parameters.

The justification of the objectives reported are the following:

Radio protection: In Ecuador has never been realized an extended campaign of measure to assess the radon risk for the population. As a consequence up today it has been not possible to know if a gas radon risk exists in this country.

About building materials, especially in the Sierra region, economic local building material are frequently used, most of them are taken from volcanic quarries, the acknowledge about exhalation rate measurement methods reported in the chapter 4 can be applied easily in Ecuador.

Regarding to water, in Ecuador is still common the use of domestic water coming from groundwater and without any treatment before the consumption; then it is fundamental the study of this kind of water sources to evaluate the risk for the population due to the radon content. The sampling and measurements proposed in the chapter 3 will be applied for this kind of measurements. In particular the new method proposed in the chapter 4 could be ideal for Ecuador.

Regarding to the indoor measurements since, a part of the Ecuadorian houses are directly in contact with the soil then an extended campaign of measurements is needed. This kind of data are the most request from international agencies.

Data Banks: Ecuador is substantially absent in the world databank, with exception of sporadic and non homogeneous data, then is urgent to compensate this lack.

Scientific research: Ecuador is a sky open laboratory for the study of the dependence of radon concentration on the environmental parameters, in particular temperature and humidity are relevant sources of radon concentration variation. In this sense Ecuador is unique and will be simple to identify areas with different climatological and environmental conditions.

5.3 Working plan

To realize the objectives proposed and taking into account the experience acquired, at least one year will be necessary to studies the main climatological, environmental, geologic, anthropization characteristics of the country and to collect all the information available from the epidemiology point of view .

All the collected information will allow to identify various representative areas of the diversity of Ecuador from the radon indoor, water and building material risk point of view. The data, methods and techniques can be tuned in those areas and the data collected will be used to design and large scale campaign of measurement. The data will be also the first contribute to the international databases.

In parallel, the information collected in the first period will allow the selection of areas of Ecuador with different climatic and environmental conditions. In those areas will be selected various kind of buildings and will be install meteorological station for correlation between environmental variation and indoor radon measurements.

Conclusions

This thesis presents measurements of gas radon concentration of activity in spring water, air indoor and of exhalation rate of volcanic building materials thanks to a new closed chamber designed and built in the Environmental Laboratory of the Physics Department of the Università della Calabria. The volcanic tuff investigated, coming from central Italy, is still widely used today as building material.

Regarding measurements on public water and taking into account the new Italian regulation (D.Lgs. 28/2016) laying down requirements for the protection of the health of the general public with regard to radioactive substances (included radon) in water intended for human consumption, we have improved the protocol of sampling and measurement in spring water. The main results obtained on spring water are listed.

1. Our protocol requires the repetitions of set of measurements for each spring one time for season and after relevant environmental events (for example after a long period of rain) before quoting an average value of concentration. This request is not present in other published protocols.
2. The emanometric techniques and the use of scintillation detectors have been preferred with respect to other commercial detectors because of the accuracy of the results obtained and of a costs/benefits assessment. A spring under observation from long time, close to the Castiglione Cosentino village, was used as a reference spring. It has on average a radon concentration of

$$(63 \pm 1)\text{Bq/l.} \tag{5.1}$$

3. The γ -spectrometry represent a valid alternative in terms of quality of the measurements in water but not in terms of costs/benefits balance for springs monitoring at large scale. The Castiglione measurement obtained with gamma spectrometry is

$$(60 \pm 2)\text{Bq/l.} \tag{5.2}$$

4. An alternative method of measurement in water is under study and consists in extracting the concentration of activity in water samples using a radon closed chamber. A preliminary result with a sample of Castiglione water is

$$(59 \pm 2)\text{Bq/l} \quad (5.3)$$

The result can be still improved and new tests with a water insertion in the chamber procedure and with samples of higher activity is underway.

Regarding to the closed chamber in Plexiglas (instead of steel) with a volume of 125 l, the use of Plexiglas makes the chamber independent from the external temperature variations and allows to use it, more easily, for studies depending on environmental parameters. Thanks to the large volume of the chamber the back diffusion effect has been negligible for all the measurements presented. One of the main parameters for the chamber characterization is the chamber leakage that for our chamber is typically, on terms of air exchange rate, below

$$0.45 \text{ l/h.} \quad (5.4)$$

The analysis of the radon exhalation rate of volcanic tuff has been performed comparing two of the possible fit techniques to evaluate chamber leakage and to extract exhalation from the radon accumulation data. Although a global fit is preferable to evaluate the chamber leakage with more precision a linear fit is sufficient and preferable to extract exhalation rate.

Regarding the exhalation rate of volcanic tuff, the samples have been intentionally chosen from scrapes of used buildings and they are with different porosity, colour and density. As expected, the exhalation measured with volcanic tuff is significantly higher with respect to others building materials and vary between

$$(0.240 \pm 0.003)\text{Bqkg}^{-1}\text{h}^{-1} \text{ and } (0.630 \pm 0.012)\text{Bqkg}^{-1}\text{h}^{-1} \quad (5.5)$$

This work, that contributes to the research about radon measurement techniques and methods, has been supported by the SENESCYT Ecuadorian program. A project to transfer the knowledge acquired in Ecuador is also presented in outline. A Collaboration with the Department of Physics of ESPOCH University of Riobamba in Ecuador is already started and a laboratory similar to ours is in preparation, a closed chamber twin to the one built, is under construction.

Acknowledgments

I would like to express my sincere gratitude to my supervisor Dr. Marcella Capua for her continuous support in my Ph.D study, for her motivation, and her guidance to obtain results of better quality. My sincere thanks also goes to Prof. Laura La Rotonda, for her support during the writing of my thesis.

A special thanks to my country, in particularly to “*Secretaría Nacional de Educación Superior, Ciencia, Tecnología e Innovación*” (SENESCYT-ECUADOR) for the financial support.

I would like to thanks to Dr. Fiorello Martire, the owner of RAD7 detector, to Dr. Anna Santaniello for the availability of the Alphaguard detector, to Eng. Giacomina Durante (ARPACAL) for the collaboration work realized with the Gamma Spectrometer and useful discussions about radionuclide in water, to Eugenio Lipreti, the technician of the Department of Physics, who helped me with the chamber built and to Prof. Rosanna De Rosa of the Department of Biology, Ecology and Earth Sciences for the building materials characterization and the useful discussions about geological aspects of Calabria.

A special thanks to my all my family. Words cannot express how grateful I am to Cristian for his inexhaustible support and encouraging.

Talía Tene Fernández
University of Calabria
February 2017

Bibliography

- [1] James L Marshall and Virginia R Marshall. Ernest rutherford, the true discoverer of radon. *Bull. Hist. Chem*, 28(2):76, 2003.
- [2] G Åkerblom, P Andersson, and B Clevensjö. Soil gas radon-a source for indoor radon daughters. *Radiation Protection Dosimetry*, 7(1-4):49–54, 1984.
- [3] Robert Bowie Owens. Thorium radiation. *The London, Edinburgh, and Dublin Philosophical Magazine and Journal of Science*, 48(293):360–387, 1899.
- [4] Ernst Dorn. Uber die von radioaktiven substanzen ausgesandte emanation. 1900.
- [5] J Mc Laughlin. An historical overview of radon and its progeny: applications and health effects. *Radiation protection dosimetry*, 152(1-3):2–8, 2012.
- [6] F Weigel. Radon. *Chem. Ztg*, 102(9):287–299, 1978.
- [7] Robert C Weast, Melvin J Astle, William H Beyer, et al. *CRC handbook of chemistry and physics*, volume 66. CRC press Boca Raton, FL, 1988.
- [8] Lawrence Stein. Chemical properties of radon. In *Radon and its decay products: Occurrence, properties, and health effects*. 1987.
- [9] Saeed A Durrani and Radomir Ilic. *Radon measurements by etched track detectors: applications in radiation protection, earth sciences and the environment*. World Scientific, 1997.
- [10] Sam Keith, John R Doyle, Carolyn Harper, Moiz Mumtaz, Oscar Tarrago, David W Wohlers, Gary L Diamond, Mario Citra, and Lynn E Barber. Toxicological profile for radon. 2012.

- [11] CEA/LNE-LNHB 2007. Nucleide - Lara library for gamma and alpha emissions, 2007.
- [12] United Nations Scientific Committee on the Effects of Atomic Radiation et al. Sources and effects of ionizing radiation, unsear report 2008. *Vol II. New York: United Nations, 20th*, 2000.
- [13] Robert C Weast, Melvin J Astle, William H Beyer, et al. *CRC handbook of chemistry and physics*, volume 69. CRC press Boca Raton, FL, 1988.
- [14] A GoWo Cameron. Abundances of the elements in the solar system. *Space Science Reviews*, 15(1):121–146, 1973.
- [15] Subhash Jaireth, Aden McKay, and Ian Lambert. Association of large sandstone uranium deposits with hydrocarbons. *AusGeo News*, 89:1–6, 2008.
- [16] AA Levinson and GL Coetzee. Implications of disequilibrium in exploration for uranium ores in the surficial environment using radiometric techniques. *Minerals Science and Engineering*, 10(1):19–27, 1978.
- [17] G Akerblom and H Mellander. 1.2 geology and radon. *Radon Measurements by Etched Track Detectors: Applications in Radiation Protection, Earth Sciences and the Environment*, page 21, 1997.
- [18] Kunihiko Kigoshi. Alpha-recoil thorium-234: dissolution into water and the uranium-234/uranium-238 disequilibrium in nature. *Science*, 173(3991):47–48, 1971.
- [19] Allan B Tanner. Radon migration in the ground: a supplementary review. *Natural radiation environment III*, 1:5–56, 1980.
- [20] William W Nazaroff. Radon transport from soil to air. *Reviews of Geophysics*, 30(2):137–160, 1992.
- [21] RL Fleischer. 1.1 radon: Overview of properties, origin, and. *Radon Measurements by Etched Track Detectors: Applications in Radiation Protection, Earth Sciences and the Environment*, page 3, 1997.
- [22] Tomozo Sasaki, Yasuyoshi Gunji, and Takeshi Okuda. Radon emanation dependence on grain configuration. *Journal of nuclear science and technology*, 41(10):993–1002, 2004.

- [23] L Morawska and CR Phillips. Determination of the radon surface emanation rate from laboratory emanation data. *Science of the total environment*, 106(3):253–262, 1991.
- [24] T DRLAM. Radon entry into buildings: Effects of atmospheric pressure fluctuations and building structural factors. 1996.
- [25] Benoit Cushman-Roisin. Environmental transport and fate. *Thayer School of Engineering Dartmouth College, University Lecture*, 2012.
- [26] JG Ingersoll. A method for measuring the exhalation of radon from building materials. *Lawrence Berkeley National Laboratory*, 2010.
- [27] Anthony V Nero and WW Nazaroff. Characterising the source of radon indoors. *Radiation Protection Dosimetry*, 7(1-4):23–39, 1984.
- [28] William W Nazaroff, H Feustel, Anthony V Nero, Kenneth L Revzan, DT Grimsrud, MA Essling, and RE Toohey. Radon transport into a detached one-story house with a basement. *Atmospheric Environment (1967)*, 19(1):31–46, 1985.
- [29] National Research Council (US) Committee on Risk Assessment of Exposure to Radon in Drinking Water. Risk assessment of radon in drinking water. (4), 1999.
- [30] Aug Pirchan and H Šikl. Cancer of the lung in the miners of jachymov (joachimstal): Report of cases observed in 1929–1930. *The American Journal of Cancer*, 16(4):681–722, 1932.
- [31] Francesco Bochicchio, Francesco Forastiere, Sara Farchi, Maria Quarto, and Olav Axelson. Residential radon exposure, diet and lung cancer: A case-control study in a mediterranean region. *International journal of cancer*, 114(6):983–991, 2005.
- [32] Daniel Krewski, Jay H Lubin, Jan M Zielinski, Michael Alavanja, Vanessa S Catalan, R William Field, Judith B Klotz, Ernest G Létourneau, Charles F Lynch, Joseph I Lyon, et al. Residential radon and risk of lung cancer: a combined analysis of 7 north american case-control studies. *Epidemiology*, 16(2):137–145, 2005.
- [33] Jay H Lubin and John D Boice. Lung cancer risk from residential radon: meta-analysis of eight epidemiologic studies. *Journal of the National Cancer Institute*, 89(1):49–57, 1997.

- [34] Jay H Lubin, Zuo Yuan Wang, John D Boice, Zhao Yi Xu, William J Blot, Long De Wang, and Ruth A Kleinerman. Risk of lung cancer and residential radon in china: pooled results of two studies. *International Journal of Cancer*, 109(1):132–137, 2004.
- [35] Sarah Darby, David Hill, Harz Deo, Anssi Auvinen, Juan Miguel Barros-Dios, H el ene Baysson, Francesco Bochicchio, Rolf Falk, Sara Farchi, Adolfo Figueiras, et al. Residential radon and lung cancer—detailed results of a collaborative analysis of individual data on 7148 persons with lung cancer and 14 208 persons without lung cancer from 13 epidemiologic studies in europe. *Scandinavian journal of work, environment & health*, pages 1–84, 2006.
- [36] Sarah Darby, D Hill, A Auvinen, JM Barros-Dios, H Baysson, F Bochicchio, H Deo, R Falk, F Forastiere, M Hakama, et al. Radon in homes and risk of lung cancer: collaborative analysis of individual data from 13 european case-control studies. *Bmj*, 330(7485):223, 2005.
- [37] GM Kendall and TJ Smith. Doses to organs and tissues from radon and its decay products. *Journal of Radiological Protection*, 22(4):389, 2002.
- [38] John B Hursh, Donald A Morcken, Thomas P Davis, and Arvin Lovaas. The fate of radon ingested by man. *Health physics*, 11(6):465–476, 1965.
- [39] Naomi H Harley and Edith S Robbins. A biokinetic model for 222 rn gas distribution and alpha dose in humans following ingestion. *Environment international*, 20(5):605–610, 1994.
- [40] National Research Council et al. *Risk assessment of radon in drinking water*. National Academies Press, 1999.
- [41] ES Robbins and NH Harley. Dose to the fetus from 222 rn in maternal drinking water. *Radioactivity in the Environment*, 7:749–755, 2005.
- [42] United Nations. Scientific Committee on the Effects of Atomic Radiation. *Effects of ionizing radiation: UNSCEAR 2006 Report to the General Assembly, with scientific annexes*, volume 2. United Nations Publications, 2009.
- [43] Glenn F Knoll. *Radiation detection and measurement*. John Wiley & Sons, 2010.
- [44] John Betteley Birks. *The Theory and Practice of Scintillation Counting: International Series of Monographs in Electronics and Instrumentation*, volume 27. Elsevier, 2013.

- [45] G De Simone, C Lucchetti, G Galli, and P Tuccimei. Correcting for h 2 o interference using a rad7 electrostatic collection-based silicon detector. *Journal of environmental radioactivity*, 162:146–153, 2016.
- [46] G Bertolini and A Coche. Semiconductor detectors. 1968.
- [47] DURRIDGE Company Inc. *RAD7 Radon detector - User manual*, 2014.
- [48] P. Tuccimei, M. Moroni, and D. Norcia. Simultaneous determination of 222rn and 220rn exhalation rates from building materials used in central italy with accumulation chambers and a continuous solid state alpha detector: Influence of particle size, humidity and precursors concentration. *Applied Radiation and Isotopes*, 64(2):254 – 263, 2006.
- [49] Saphymo GmbH. *AlphaGUARD. The reference in professional radon measurement*, 2009.
- [50] Pylon Electronic Development Company ltd. *Continuous passive radon detector. Instruction Manual. Rev 0*, 1989.
- [51] Robert W Ramsey Jr and Payasada Kotrappa. Electret ion chamber for radon monitoring, February 12 1991. US Patent 4,992,658.
- [52] P Kotrappa, JC Dempsey, JR Hickey, and LR Stieff. An electret passive environmental 222rn monitor based on ionization measurement. *Health Physics*, 54(1):47–56, 1988.
- [53] P Kotrappa, JC Dempsey, RW Ramsey, and LR Stieff. A practical e-permtm (electret passive environmental radon monitor) system for indoor 222rn measurement. *Health Physics*, 58(4):461–467, 1990.
- [54] mi.am s.r.l. *RAD ELEC E-PERM Sistema per la misura del gas radon. Manuale d’uso*, 2008.
- [55] Rad Elec Inc. *SPER-1E User’s manual*.
- [56] DURRIDGE Company Inc. *RAD H2O User manual - Radon in water accessory*, 2014.
- [57] Howard M. Prichard. The transfer of radon from domestic water to indoor air. *Journal (American Water Works Association)*, 79(4):159–161, 1987.
- [58] K. Freyer, H.C. Treutler, J. Dehnert, and W. Nestler. Sampling and measurement of radon-222 in water. *Journal of Environmental Radioactivity*, 37(3):327 – 337, 1997.

- [59] Maria Chiara Angiochi. Protocollo di misura e analisi dati di concentrazione di radon acqua, 2010/2011.
- [60] Interpretation of radon anomalies in seismotectonics and tectono-gravitational analyses: the se portion of the crati graben (northern calabria, italy). *Tectonophysics*, page 396, 2005.
- [61] Jonathan C H Miles. Temporal variation of radon levels in houses and implications for radon measurements strategies. *Radiation Protection Dosimetry*, 93(4):369–375, 2001.
- [62] F Bochicchio, G Campos-Venuti, S Piermattei, C Nuccetelli, S Risica, L Tommasino, G Torri, M Magnoni, G Agnesod, G Sgorbati, et al. Annual average and seasonal variations of residential radon concentration for all the italian regions. *Radiation Measurements*, 40(2):686–694, 2005.
- [63] Akihiro Sakoda, Yuu Ishimori, and Kiyonori Yamaoka. A comprehensive review of radon emanation measurements for mineral, rock, soil, mill tailing and fly ash. *Applied Radiation and Isotopes*, 69(10):1422–1435, 2011.
- [64] RL Fleischer. 1.1 radon: Overview of properties, origin, and transport. 1997.
- [65] P Tuccimei, M Moroni, and D Norcia. Simultaneous determination of ^{222}Rn and ^{220}Rn exhalation rates from building materials used in central italy with accumulation chambers and a continuous solid state alpha detector: influence of particle size, humidity and precursors concentration. *Applied Radiation and Isotopes*, 64(2):254–263, 2006.
- [66] Christopher YH Chao, Thomas CW Tung, Daniel WT Chan, and John Burnett. Determination of radon emanation and back diffusion characteristics of building materials in small chamber tests. *Building and Environment*, 32(4):355–362, 1997.
- [67] NP Petropoulos, MJ Anagnostakis, and SE Simopoulos. Building materials radon exhalation rate: Erricca intercomparison exercise results. *Science of the total environment*, 272(1):109–118, 2001.
- [68] G Sappa, G Giglio, and G De Casa. Mechanical characteristics of some volcanic tuffs used in the buildings of ancient rome. In *MRS Proceedings*, volume 352, page 733. Cambridge Univ Press, 1995.

- [69] MD Jackson, Fabrizio Marra, RL Hay, C Cawood, and EM Winkler. The judicious selection and preservation of tuff and travertine building stone in ancient rome. *Archaeometry*, 47(3):485–510, 2005.
- [70] Serena Righi and Luigi Bruzzi. Natural radioactivity and radon exhalation in building materials used in italian dwellings. *Journal of Environmental Radioactivity*, 88(2):158–170, 2006.
- [71] Nabil Hassan, Tetsuo Ishikawa, Masahiro Hosoda, Atsuyuki Sorimachi, Shinji Tokonami, Masahiro Fukushi, and Sarata Sahoo. Assessment of the natural radioactivity using two techniques for the measurement of radionuclide concentration in building materials used in japan. *Journal of radioanalytical and nuclear chemistry*, 283(1):15–21, 2009.
- [72] B Capaccioni, G Cinelli, D Mostacci, and L Tositti. Long-term risk in a recently active volcanic system: Evaluation of doses and indoor radiological risk in the quaternary vulsini volcanic district (central italy). *Journal of Volcanology and Geothermal Research*, 247:26–36, 2012.
- [73] Marco Mancini, Odoardo Girotti, and Gian Paolo Cavinato. Il pliocene e il quaternario della media valle del tevere (appennino centrale). *Geologica Romana*, 37(2003-2004):175–236, 2004.
- [74] Dan-Gabriel Calugaru and Jean-Marie Crolet. Identification of radon transfer velocity coefficient between liquid and gaseous phases. *Comptes Rendus Mecanique*, 330(5):377–382, 2002.
- [75] Daniel Marcos Bonotto and JN Andrews. Transfer of radon and parent nuclides ^{238}U and ^{234}U from soils of the mendip hills area, england, to the water phase. *Journal of Geochemical Exploration*, 66(1):255–268, 1999.
- [76] Joash N Ongori, Robert Lindsay, and Mashinga J Mvelase. Radon transfer velocity at the water–air interface. *Applied Radiation and Isotopes*, 105:144–149, 2015.
- [77] "Bolivar Education" Foundation. Volunteer work in ecuador.
- [78] Mapas y fotos satelitales del mundo.
- [79] JF Marquez. El planeta azul, url = <http://jfbblueplanet.blogspot.it/2012/11/volcanes-de-america-del-surmapas.html>, lastchecked = 08.02.2017.

- [80] Norman Myers, Russell A Mittermeier, Cristina G Mittermeier, Gustavo AB Da Fonseca, and Jennifer Kent. Biodiversity hotspots for conservation priorities. *Nature*, 403(6772):853–858, 2000.
- [81] RA Mittermeier, CG Mittermeier, TM Brooks, JD Pilgrim, WR Konstant, Gustavo AB Da Fonseca, and C Kormos. Wilderness and biodiversity conservation. *Proceedings of the National Academy of Sciences*, 100(18):10309–10313, 2003.
- [82] Judith Kimberling. Indigenous peoples and the oil frontier in amazonia: The case of ecuador, chevrontexaco, and aguinda v. texaco. *NYUJ Int'l. L. & Pol.*, 38:413, 2005.